UNIVERSITY OF CALIFORNIA, SAN DIEGO

# A geophysical and biological characterization of the Rose Canyon Fault's constraint on sediment budget and biohabitats

A Thesis submitted in partial satisfaction of the requirements
for the degree Master of Science

in

Oceanography

by

Ryan David Switzer

Committee in charge:

James Leichter, Chair
Ed Parnell
Neal Driscoll

2014

The thesis of Ryan David Switzer is approved, and it is acceptable in the quality and form for publication on microfilm and electronically:

_____

_____

_____

Chair

University of California, San Diego

2014

# DEDICATION

I would like to dedicate this thesis to Paul and Barbara Peterson. They have raised me as if I was their own child. I feel so lucky to have been raised by such caring and loving individuals who have made a huge impact in both my personal and academic life. Their continued support and encouragement has driven me to succeed and without them I would not be where I am today.

TABLE OF CONTENTS

LIST OF FIGURES

LIST OF TABLES

# ACKNOWLEDGMENTS

I would like to acknowledge Dr. Ed Parnell for his help in the field, analysis of data. I thank him for the many hours he spent in the field collecting data, his assistance with processing and analyzing ROV data, as well as his role in publishing.

I would also like to acknowledge Dr. James Leichter for his assistance in editing and his role in mentoring in both my academic and research throughout my time here at Scripps Institution of Oceanography. I would also like to acknowledge his assistance in publishing our results.

Dr. Neal Driscoll was instrumental in making this project happen by supplying me with both CHIRP seismic and multibeam swath bathymetry of the study area. I would also like to thank Neal for hiring me in his lab upon graduation from UCSB.

ABSTRACT OF THE THESIS

A geophysical and biological characterization of the Rose Canyon Fault's constraint on sediment budget and biohabitats

by

Ryan David Switzer

Master of Science in Oceanography

University of California, San Diego, 2014

Professor James Leichter, Chair

Ecological processes are modulated by the patch structure of soft and hard bottoms within continental shelf ecosystems. This patch structure is partly a result of the interaction between geological and hydrodynamic controls on sediment allocation, and to some degree by the production of biogenic habitat. Increased habitat patchiness and fragmentation affect the species richness and biological community structure, and potentially modulate trophic dynamics.

Past tectonic and oceanographic processes have altered the geomorphology and local hydrodynamics of the narrow continental shelf in the La Jolla region. The obliquity in the strike-slip of the Rose Canyon Fault (RCF) has led to a rich tapestry of heterogeneous benthic environments due to the shoaling of the transgressive surface which controls the allocation of modern Holocene sediments along the shelf.

In this study, I surveyed the benthos and habitat along previously conducted seismic sub-bottom profiles (Compressed High Intensity Radar Pulse - CHIRP) using a remotely operated vehicle (ROV) in order to groundtruth seismic and multibeam swath bathymentry and to characterize biological habitat associations. This study elucidated the role of the relief of the transgressive surface in allocating sediment along the continental shelf and how the shoaling of the transgressive surface along strike occurs concomitantly with decreases in sediment thickness, leading to (1) increased patchiness and habitat fragmentation and (2) increased edge habitat and species richness.

.

## Introduction

The offshore region of La Jolla is a rich and diverse ecosystem, sustaining a large number of species, within a tectonically active geologic setting. Compressed high intensity radar pulse (CHIRP) seismic data, multibeam swath bathymetry, and observations collected with a remotely operated vehicle (ROV) were used to document and characterize this understudied habitat. These combined data produce a better understanding of the biophysical interactions affecting the ecosystem through the interactions of tectonics, local circulation, and control of habitats through sedimentation and erosive processes. The results of this study further our understanding of this habitat and possible value of extensions of current marine protected areas (MPAs) to incorporate portions of the exposed hardground associated with the Rose Canyon Fault (RCF).

The topography and bathymetry of the La Jolla region is greatly altered by active strike-slip faults and deep submarine canyons (Figure 1). This geomorphology results in extensive spatial heterogeneity and localized exposure of hard substrate on the seafloor, leading to a patchy framework of benthic habitats. A benthic habitat is described as a contiguous geographical region where the physical, chemical, and biological environment is decidedly disparate from the surrounding environment (Kostylev et al., 2001). The continental shelf accounts for roughly 15% of the sea bed, yet displays high topographical heterogeneity marked by pronounced environmental gradients, as well as tectonic processes that in conjunction with one another create an array of habitats for a large number of biological communities (Levin et al., 2001).

The combination of strong water column density stratification and offshore generation of internal waves in the region produces strong microhabitat variability in near-bottom physical conditions affecting organismal distributions. The interaction of internal waves with geomorphological structural heterogeneity can strongly influence the physical and chemical environment across an array of complex nearshore ecosystems, from high productivity kelp forests to filter feeding communities dominated by soft corals on shelf slopes. The high bathymetric relief in the study area provides the necessary conditions for soft coral habitat: hard substrate and accelerated bottom currents, essential for the flux of particles, delivery of larvae, removal of waste and excess sediment. Deep-water corals have been receiving attention because of the increased diversity and abundance of associated organisms relative to the surrounding deep sea, and because of their vulnerability to human impact (Cimberg et al., 1981; Mortensen, 2001)

The deep canyons in the vicinity of the study area are highly eroded and therefore not laden with sediments. These canyons are likely to generate locally strong currents, resuspension and mixing, which is critical for the corals to thrive. Gorgonian soft corals are sessile, long-lived, slow-growing, filter feeding, ecosystem engineers that provide critical nursery habitats for many fish and invertebrate species (Buhl-Mortensen et al., 2010; Pirtle, 2005). However, the interactions of geomorphology with physical oceanography that drive the ecology of these key foundation species in shelf slope habitats are poorly understood. The exploration of this study area to determine the ecology and occurrence of the soft corals is necessary to support the conservation and

long-term protection of these coral populations along the San Diego shelf and continental shelves globally. We combine geophysical methods with a biological perspective to characterize organism-substrate interactions and relationships (Diaz et al.,, 2004). The shelf region offshore of Torrey Pines State Reserve lacks initial descriptive baseline studies reinforcing the importance of identifying physical features and an inventory of species and their associated habitats. This baseline work will allow for manipulative, integrative experiments as well predictive modeling of causal mechanisms across the region to be developed (Engle et al., 1995). We focused on the changes to structural diversity and associations of foundation species as along strike of the RCF.

This study describes how tectonic deformation along the RCF modifies rocky habitats, sediment dispersal and biological utilization of habitats. Special attention is paid to invertebrate communities that have the morphological ability to add structure and complexity to the physical habitats, thereby creating additional three-dimensional structure for fish and other invertebrates to utilize for shelter, nursery grounds, and other needs (Buhl-Mortensen et al., 2010; Pirtle, 2005). We attempt to discover associations of fish with secondary biogenic structure-forming invertebrates as they are a biological component of habitat and community structure due to their size and complex anastomosing morphology (Buhl-Mortensen et al., 2010; Pirtle, 2005). We also describe how high habitat fragmentation increases edge habitat and therefore edge effect and trophic dynamics. Conservation of biodiversity in the form of a functioning ecosystem requires protection of diverse habitats at the appropriate scale (Ierodiaconou et al., 2011).

## Study Area

### Geological Setting

In southern California, tectonic deformation between the Pacific and North American Plates is accommodated primarily by a zone of strike-slip faults, with maximum deformation along the San Andreas system, decreasing westward towards the offshore inner Continental borderland region (Grant & Shearer, 2004; Walls et al., 1998). The San Diego area is characterized by a series of sub parallel, en echelon faults including, from east to west, the San Jacinto, Elsinore, and Newport-Inglewood-Rose Canyon fault zones (Hogarth et al., 2007). The Newport-Inglewood fault zone (NIFZ) is the easternmost northwest-southeast trending fault zone that characterizes the California borderlands (Fischer & Mills, 1991; Wright, 1991). Approximately 10 km offshore southern California there is region of faults that connect the NIFZ with the Rose Canyon fault zone (RCFZ) (Grant & Shearer, 2004). The RCFZ in San Diego has many "well-expressed geomorphic characteristics of an active strike-slip fault, including scarps, offset and deflected drainages and channel walls, pressure ridges, a closed depression and vegetation lineaments" (Lindvail & Rockwell, 1995). Figure 2 displays regions in which transpression and extension have occurred around RCF jogs due to the obliquity of the dextral strike-slip fault (Le Dantec et al., 2010). Two of these localized areas of uplift are evident in the topography of Mt. Soledad and the bathymetry and sub-bottom structure offshore of Torrey Pines State Reserve (Le Dantec et al., 2010; Hogarth et al., 2007).

The localized pop-up ridge located offshore of the Torey Pines State Reserve is a transpressional region where the dextral motion of the strike-slip fault is interrupted by a

non-planar, oblique, westward step-over leading to localized uplift (Le Dantec et al., 2010) (Figure 2). This transpressional region, pop-up structure, evident in both multibeam bathymetry and CHIRP seismic profiles, is correlated with the deflection of bathymetric contours offshore at water depths greater than 60 m (Hogarth et al., 2007). The nearshore contours in this region are not marked by this landward deflection of isobaths even though the slope of the sediment thickness contour lines, isopach surface, change in this area from west dipping to southwest dipping (Hogarth et al., 2007; Orange, 1999; Driscoll and Hogg, 1995). Hogarth et al., (2007) hypothesize that this pop-up structure, created by the constraining left step-over within the RCF plays an important role in the preservation of sediments on the local nearshore shelf region. Wave-cut notches are observed along the continental shelf in the transgressive surface, recording past still stands in eustatic sea level. The transgressive surface is the flooding surface that separates the underlying lowstand systems tract from the overlying transgressive systems tract (Nummedal & Swift, 1987). In the past 20 kya, eustatic sea level has risen approximately 125 m at fluctuating intervals to its current level (Fairbanks, 1989; Emery, 1958; Byrd et al., 1975; Henry, 1976; Waggoner, 1979; Darigo & Osbourne, 1986). Some of the relief on the transgressive surface has been, and still is modified, by wave-based erosion in the nearshore (Le Dantec et al., 2010). Wave-based erosion enhances the smoothness of the seafloor as coarse-grained sediments eroded from the shoreface are transported to the bathymetrical low areas offshore, thereby eroding the highs and filling in the lows (Le Dantec et al., 2010). This fault induced roughness in the transgressive surface is preserved in deeper water because these areas were more rapidly transgressed during the most recent interglacial, such as meltwater pulse 1A (mwp-1A) (Fairbanks,

1989). The locations of healing-phase deposits is largely a consequence of the varying rates of sea level rise and melt water pulses, during the last sea level transgression (Fairbanks, 1989). This is evidenced in CHIRP seismic profiles, which display a great deal more surface rugosity of the transgressive surface as well as the presence of a sedimentary basal unit which infill the structural lows of the transgressive surface on the outer shelf (Le Dantec et al., 2010). With decreasing rates of sea-level rise, the nearshore portion of the continental shelf is exposed to wave-based erosion over a longer period and existing structural features were smoothed and effectively leveled (Le Dantec et al., 2010). This pattern of increased rugosity offshore is likely enhanced by the overprinting of erosion during several sea level cycles (Le Dantec et al., 2010). Because tectonic deformation of the RCF occurs shore-parallel, we can discern the tectonic signal from the glacial-eustatic fluctuations from regional tectonic uplift (Hogarth et al., 2007; Kennedy, 1975). This may further our understanding how tectonics regulate sediment dispersal and preservation on the shelf.

Outside the two areas of uplift due to the RCF, there is no bedrock exposure offshore of La Jolla between the mid-shelf wedge and the beach, thereby limiting hard ground exposure and possible sessile filter feeder rocky habitats (Le Dantec et al., 2010). Compressed High Intensity Radar Pulse (CHIRP) instrumentation was used along the RCF to obtain high resolution imagery of the nearshore and subsurface stratigraphy to a subsurface depth of 70 –100 m in fine sediments, and 10-20 m depth in consolidated hardgrounds. The amplitude of the stratigraphic reflectors in CHIRP profiles is controlled by the contrasting acoustic impedance, the bulk density of the medium times the velocity of the signal within the medium, between stratum (Rentz, 2010). CHIRP seismic profiles

give insight into the subsurface stratigraphy, which can be inferred from the shoreline exposure of the geologic formations in the sea cliffs of Torrey Pines State Reserve (Le Dantec et al., 2010; Lindvall & Rockwell, 1995; Rentz, 2010). The pop-up structure offshore of the Torrey Pines State Park influences the hydrodynamics, sediment preservation on the inner shelf, and biohabitat partitioning and utilization.

The sedimentary and morphological evolution of continental margins depends on three main factors (Christie-Blick & Driscoll, 1995; Posamentier & Allen, 1999):

1) Eustasy
2) Sediment supply
3) Tectonic deformation

Discerning how these parameters affect sediment accumulation is often difficult when the factors are operating at different spatial scales (Sommerfield & Lee, 2003, 2004).

The localized deformation of the Torrey Pines pop-up structure affects the relief of the transgressive surface, which plays an important role in sediment allocation, erosion and deposition, on the inner continental shelf. The Torrey Pines pop-up structure is located at the southern end of the Oceanside littoral cell. The Oceanside Littoral Cell predominantly transport of sediments in a southerly direction from Dana Point to La Jolla (Inman & Chamberlain, 1960). The RCFZ separates Cretaceous lithified rocks to the south from poorly cemented Eocene sands and gravels to the north, and lines up with the La Jolla Canyon (Le Dantec et al., 2010). The La Jolla and Scripps Canyon heads extend into shallow water (8–10 m) and as such they modify nearshore circulation, surface wave patterns, and littoral sediment transport (Shepard & Inman, 1950; Thomson et al., 2005).

The sediment thickness exhibits a wedge-shaped cross-shore profile with a mid-shelf depocenter (Byrd et al., 1975; Henry, 1976; Hogarth et al., 2007). A depocenter is an area that exhibits the thickest deposition in a sedimentary basin and is tectonically controlled through displacement of the transgressive surface. Figure 3 displays the thinning of sediment thickness along strike to the north of the Scripps Canyon, and dip lines show that maximum sediment thickness above the transgressive surface is located on the midshelf and diminishes both landward and seaward (Hogarth et al., 2007). Sediment input mostly consists of sand and silt derived from river discharge to the north and widespread cliff erosion (Stow & Chang, 1987; Hass, 2005; Young & Ashford, 2006).

The main sources of inner shelf sediment in the Oceanside Littoral Cell are derived from the Santa Margarita and San Luis Rey rivers, as well as erosional reworking of the sea cliffs, gullies, and terrace surface erosion (Young et al., 2010). Urbanization and coastal seawall armoring have greatly altered the coastline and reduced both fluvial and seacliff sediment sources (Young et al., 2010). In the Oceanside Littoral Cell, damming has reduced the river sediment input by approximately 50% (Flick, 1993, 1994; Willis & Griggs, 2003), while coastal armoring and segregation have largely eliminated a significant portion of sea cliffs as a potential sediment source (Young et al., 2010). The sea cliffs are generally composed of two geologic units:

(1) A lower unit of lithified Eocene, Miocene, or Pliocene mudstone, shale, sandstone, and siltstone.

(2) An upper unit of unlithified Pleistocene terrace deposits (Kennedy, 1975; Young et al., 2010).

Torrey Pines State Reserve sea cliffs exhibit Torrey Pines sandstone overlying the Del Mar shale formation, both of which are early Eocene deposits (Kennedy, 1975; Young et al., 2010) The Del Mar Formation is a fine-grained shale, compacted and reinforced through the dissolution of biogenic $CaCO_3$ which acts to bolster its integrity and resistance to deformation (Kennedy & Moore, 1971). Nearshore sediment deposition is controlled through wave dispersal, whereas, the offshore region is controlled by the sedimentary budget, leading to maximal deposition in the mid-shelf region.

**Ecological Setting**

The La Jolla region contains a heterogeneous physical environment that supports diverse biological assemblages. The most conspicuous organisms present in the hardgrounds of La Jolla are filter feeding gorgonians. These gorgonians *Adelogorgia phyllosclera*, *Leptogorgia chilensis*, *Eugorgia rubens*, *Muricea fruticosa*, and *Muricea californica*, lack symbiotic zooxanthellae, and are therefore restricted to two feeding strategies: active transport of dissolved nutrients across epidermal membranes, and suspension feeding (Muscatine, 1973; Johannes, 1974; Lewis & Price, 1975, 1976). As passive suspension feeders, gorgonians are highly reliant upon the velocity of ambient currents to move particle-laden fluids through their colonial feeding polyps which are dependent on the hydrographic regime influenced by bottom bathymetrical features (Sponaugle, 1991).

There is a balance between fluid velocity and particle capture. At reduced flow, encounter rate of particles is minimized, whereas at high fluid velocities, mechanical deformation of the colonial structure may occur, causing increased difficulty in both

encounter rate and capture of food particles (Sponaugle, 1991). Particle encounter and capture therefore is likely maximized at an intermediate range of flow speeds (Sponaugle, 1991). Flow velocities in the vicinity of the polyps can be kept relatively constant through the reversible deformation of the colony which may account for the broad range of habitats and fluid velocities gorgonians inhabit (Sponaugle & LaBarbera, 1991). Gorgonians also provide a complex, 3-dimensional secondary biogenic structure that can be utilized by a variety of habitat-dependent fish and invertebrates (Buhl-Mortensen et al., 2010). The interactions of geomorphology with physical oceanography that drive the ecology of these key foundation species in shelf slope habitats are poorly understood.

## Methodology

Both CHIRP seismic profiles and multibeam swath bathymetry were used to select a region of the inner shelf that appeared to be most impacted by tectonic deformation associated with segmentation along the RCF. The area we chose encompassed what Hogarth et al., (2007) termed the Torrey Pines pop-up structure offshore of the Torrey Pines State Reserve. A remotely operated vehicle (ROV), SeaBotix little benthic vehicle (LBV) 150, was used to groundtruth both seismic and bathymetrical data and to observe biological community associations with habitat structure, sediment thickness, and bathymetrical features. The ROV footage was then analyzed using the classification scheme presented in Table 2 and combined with CHIRP seismic data and multibeam swath bathymetry to relate underlying tectonic, sedimentary, and hydrographic forces to the biological community associations among the heterogeneous benthic habitat framework.

### Procedures and Data Collection

A SeaBotix LBV 150, remotely operated vehicle (ROV), was operated from an 8 m twin-outboard boat to survey the benthic species assemblages and physical environment along replicated transects. The ROV field operations consisted of replicating three of the cross shore CHIRP transects, displayed in Figure 2, encompassing the Torrey Pines pop-up structure. The three cross shore CHIRP lines selected were labeled CHIRP 3, CHIRP 5, and CHIRP 7. The start and end points for the ROV transects were taken directly from the ship file corresponding to the CHIRP seismic survey. Table 1 shows the

coordinates, from south to north that were entered into the ships onboard navigation system.

Table 1. Coordinates entered into onboard ship GPS for replicating CHIRP transects during ROV survey.

| CHIRP Line | Date | Start Point (Lat/Long) | End Point (Lat/Long) |
|---|---|---|---|
| 3 | 10/21/2013 | 32°55’8.44 N<br>117°18’35.58 W | 32°55’51.27 N<br>117°16’54.49W |
| 5 | 01/25/2014 | 32°56’19.5 N<br>117°17’9.35 W | 32°55’30.04 N<br>117°19’1.95 W |
| 7 | 08/14/2013 | 32°55’57.0 N<br>117°19’14.31 W | 32°56’44.44 N<br>117°17’23.28 W |

Each ROV transect was performed on separate days 8/14/2013 (CHIRP 7), 10/21/2013 (CHIRP 3), and 01/25/2014 (CHIRP 5). The preparation and execution were reproduced in order to maximize comparability between ROV transects. The date and time on the SeaBotix LBV 150, supplemental GoPro high-definition camera, SeaBird conductivity, temperature, depth recorder (CTD), as well as the boat GPS file were all synchronized prior to beginning the survey. A Hemisphere V110 GPS, sample rate 10 Hz (10 positions per second) was run using Fugawi software which was set to record points when separation reached 5 m. The ROV was then attached to a 200 m fiber optic cable which was run through a pulley system attached to a rotating davit at the stern of the boat.

A 20 kg clump weight was attached to a leader line 20 m from the attachment of the ROV. The clump weight allowed us to position the ROV approximately 1 m off the sea floor. The SeaBotix LBV 150 with attached SBE 37-SMP MicroCAT CTD recorder, and the 20 kg clump weight were placed overboard between 20-40 m depth. The SBE 37-SMP MicroCAT CTD records oxygen (in ml/L), conductivity, temperature (°C), and depth (m) at one minute intervals, internally within the device. Once the ROV reached the seafloor we proceeded along the transect using onboard navigation system at a speed of 1-3 km/h. Live feed video data was sent to the ROV operator on board the vessel via the fiber optic cable. Notes were recorded on a tablet describing the physical setting of the benthic environment as well as species identifications. The ROV camera and electronics recorded the tracked azimuth, current water depth in meters (m), temperature in degrees Celsius (°C), date and time electronically on an onboard laptop, which was converted from an analog to a digital signal using a Canopus ADVC110 digital video converter.

### Video Analysis

In a preliminary view of each video transect date, time, and depth at which either the visible composition, relative grain size, bedform, or slope changed were recorded. In addition the time and depth at which the ROV crossed an isobath that was a multiple of 10 m were recorded. This provided a list of times at which changes in the substrate and depth occurred from start to finish of each transect, allowing segments to be placed into separate bins. The recorded date and time at which the substrate changed or an isobath of a multiple of 10 m was crossed represents the start of a new bin and the end of the

previous bin. The differences between start and end times of each habitat segment recorded in the preliminary view were multiplied by 10 random decimals between 0 and 1, using a random number generator in Microsoft Excel, and then added to the start time. From this list of ten times the first five that had at least a five second difference between start and end times were chosen to represent an individual bin to be analyzed. This process was repeated until all depth-bins contained up to five non-overlapping start times. Each time within the individual bins represents the start time for a five second snippet of video that were analyzed using the categorical and numerical criteria shown in Table 2.

Table 2. Categorical and numerical variables documented along ROV transects.

| |
|---|
| • Start Time, End time, ROV depth, ROV temp, |
| • Composition (Soft, Sediment Veneer 3:1 ratio, Rocks with Sand 1:3 ratio, Boulder) |
| • Relative angle (Flat or Sloping) |
| • Grain size (Coarse, fine, mud, or none) |
| • Bedform (smooth, linguloid ripples, hatched ripples, parallel waves, parallel ripples) |
| • Floor Snow (snowy peaks, light snow dust) |
| • Other Bed characteristics (Diatoms and Shell hash) |
| • Mound type- Small and large mounds. |
| • Hole type- quantity all linearly numeric except pits which were $\log_4$ (small, pits, octopus den, ditch) |
| • Squid mops ($\text{Log}_4$) |
| • Sea Snow- Light and heavy (Li, Hv) Small and Large (Sm, Lg) or not present (NP) |
| • Turf Algae (microalgae on sediment or rocks) 1= very sparse 2= intermediate 3= covered |
| • Macroalgae (1= very sparse 2= intermediate 3 =covered) Py-Phyllospadix, Mc-Macrocystis pyrifera, Sg-Sargassum, Ee-Eelgrass, Ma-unknown drift algae , Eg- Egregia, Pe-Pelagophycus. |
| • Drift algae to species level (1=very sparse 2= intermediate 3=covered) |
| • Quantitative measure of organismal abundance, to species level when possible. |

**Data Processing**

Processing of the video data began by grouping individual video snippets into bins based on the 14 variables listed in Table 3. We then separated the physical variables displayed in Table 3, from their respective biological organism counts. The four physical variables, composition, grain size, bedform, and relative slope, were put through a multiple correspondence analysis (MCA) to discern relationships among independent categorical variables. The loading coefficients from the MCA were then plotted along each of the four dimensions from the MCA to visualize habitat variability. MCA loading coefficients were then combined with their respective biological organism counts in order to perform a redundancy analysis. The MCA loading coefficients were used to constrain the biological organism data in the redundancy analysis (RDA). Results from the redundancy analysis were plotted demonstrating organismal vector habitat associations with constraining MCA loading coefficients. MCA loading coefficients allowed us to numerically categorize substrate variability along each ROV transect while the RDA uncovered organismal habitat associations.

Because the boat was traveling 1-3 km/h, the track lines were often not straight due to wind and currents. Therefore distance from the origin of the transect and observation points were calculated from each video segment location to the origin of each transect. Distances were calculated by first converting latitude and longitude into a universal transverse mercator (UTM) projection. A UTM projection uses the “central meridian” drawn between the poles to subdivide the Earth into separate zones in a two-dimensional Cartesian coordinate system. The central meridian was used to set up the

origin for the grid, which then allowed for points to be described by their distance and angle from the origin. Video segments were then organized by increasing distance from the origin. These calculated distances were then merged with the categorical data used to describe the physical setting of the environment using the nominal variables shown in Table 3.

Table 3. Four categories of physical descriptive variables used to characterize physical substrate of habitats and for MCA.

| **Composition** | **Relative Angle** | **Grain** | **Bedform** |
|---|---|---|---|
| Boulder | Flat | Coarse | Hatched ripples |
| Rocks with sand | Slope | Fine | Linguloid ripples |
| Sediment veneer | | Mud | Outcrop |
| Soft | | None | Smooth |

These data were then analyzed using R (R Core Team, 2012). A multiple correspondence analysis (MCA) was performed on the nominal categorical data describing the physical environment of the ROV transects. MCA reveals frequency-based associations among categorical data for exploratory purposes and does not determine significance or discern relevance. MCA allowed for detection of underlying structures within a nominal categorical data set. Each data point was represented as a point in a low-dimensional Euclidean space. In an MCA, an indicator matrix was created in which the rows represent the individual changes in substrate as a function of distance from the

transect origin, whereas the columns represent nominal categorical variables (Legendre & Legendre, 2012). Associations between variables were calculated by calculating the chi-square distance between the different categorical variables and individual observations. Frequencies of co-occurrence are converted to distances, which can then be viewed in Euclidean space by computing eigenvectors of the correlation matrix. These frequency-based associations are determined using coefficient scoring factors of the coordinates of the column vertices, with one for each level of each factor (Legendre & Legendre, 2012). The values or scores are coefficients that indicate how much each original variable contributes to the linear combination forming this component (Legendre & Legendre, 2012). The further that each coefficient is from zero in the positive direction, the greater contribution that variable makes to the component (Legendre & Legendre, 2012). Component loadings are simple correlations (using Pearson's *r)* between the components (i.e. component scores for each object) and the original variables (Legendre & Legendre, 2012). High loadings indicate that a variable is strongly correlated with, and thus strongly loads on, a particular component whereas negative loadings indicate an inverse correlation with a particular component. The first axis is the most important dimension, in terms of describing the proportion of total variance accounted for followed by the second, third, and fourth dimensions (Quinn & Keough, 2002).

The four factors displayed in Table 3 were used in the MCA with a total of 211observations from the three ROV transects. The subcategories of sedimentary soft substrate composition are: S1 (Coarse), S2 (Fine), and M (Mud/Finest). Sediment veneer (SV), rocks with interstitial sand (RS), and boulders (B). All habitats relative angles were

categorized as flat unless they exceeded 5 m of relief, in which case they were categorized as sloping. The grain sizes were labeled as either S1 (Coarse), S2 (Fine), and M (Mud/Finest), or none if exposed hardgrounds lacked interstitial sediment. The fourth categorical variable, bedforms, was described using four sub-variables. Smooth was used to define habitats that lacked any organization or repetition of bedforms. The other sedimentary bedform categories are hatched ripples, linguloid ripples, parallel ripples and parallel waves. Sediment veneer, boulder, and rocks with sand habitats were all categorized as outcrops. In the MCA model, all depths within 10 meter interval bins were assigned median values, for example depths ranging from 40-50 m were given the depth 45 m.

**Redundancy Analysis**

MCA 1, 2, 3, and 4 component loading scores, and 65 distinct groups of organism counts from each video segment were combined into a matrix. Video segments that totaled zero organismal data points were removed from matrix, resulting in a total of 520 individual observations with 69 distinct response variables. MCA loading scores represent our explanatory variable which was used to constrain our 65 distinct species groups, the response variable. A redundancy analysis (RDA) was performed on the resultant matrix using the Vegan package in R. The organism counts were standardized to zero mean and unit variance prior to RDA, because organismal abundances were not dimensionally homogenous as some organisms were counted in $\log_4$. RDA is a statistical procedure used to estimate variance and develop predictive modeling by constraining the response variables by explanatory variables. It applies a linear regression and represents

response variables as a linear function of explanatory variables and then uses a principle component analysis to visualize the resultant in a biplot (Legendre & Anderson, 1999). A complete description of RDA is given in Van den Wollenberg (1977), Legendre and Legendre (2012), and Legendre and Anderson (1999).

To display sites and species in a two-dimensional biplot, RDA 1 eigenvalues were plotted against RDA 2 eigenvalues for all of the organismal data using a scaling of 3 (scaling = 3). This plots and scales the species and site data symmetrically by the square root of the eigenvalues (Legendre & Legendre, 2012). The biplot is displayed as a point vector plot where the sites, are displayed as points, while species, are represented by vector lines drawn from the origin (Digby & Kempton, 1987; Legendre & Legendre, 2012). The directionality and relative length of organismal vectors is important in describing site correlations and species abundances. Small angles between sites and organismal vectors suggest high positive correlations; while arrows pointing in opposite directions connote negative correlations (Legendre & Anderson, 1999) Increasing vector length implies increasing species abundances in that direction (Legendre & Anderson, 1999).

### Clustering Around Medoids

The different habitats were clustered, using a partitioning, into 7 clusters around the medoids. This was performed in R using the Library (Vegan) diversity function-Ecological Diversity Indices and Rarefaction Species Richness. The partitioning around medoids (PAM) minimizes a sum of dissimilarities providing a silhouette plot. After finding a set of k-medoids, k-clusters are constructed by assigning each observation to the

nearest medoid. The goal is to find, k, representative objects which minimize the sum of the dissimilarities of the observations to their closest representative object (Legendre & Legendre, 2012).

### CHIRP Methods

CHIRP survey procedures are described in detail in LeDantec et al. (2010) and Hogarth et al., (2007). The relevant steps are briefly described below.

In 2002 and 2003, high resolution swath bathymetry and compressed high intensity radar pulse (CHIRP) seismic data were acquired offshore Torrey Pines State Reserve north to the Penasquitos Lagoon (Figure 2). Both SwathPlus-L (formerly Submetrix) interferometric swath bathymetric sonar by SEA Ltd (http://www.sea.co.uk) and the Scripps sub-bottom reflection sonar system (SUBSCAN), which is a modified EdgeTech (http://www.edgetech.com/) CHIRP system that consists of a dual-transducer X-Star sonar with an ADSL link from the towfish to the topside computers were used. The CHIRP sonar (Edgetech) swept with a frequency of 1-5.5 kHz which yields sub-meter resolution. The CHIRP seismic system was mounted on a surface tow frame with a mounted global positioning system (GPS) receiver, and was complemented with an onboard motion sensor and GPS receiver to measure both attitude and position (Le Dantec et al., 2010). An isopach map was created by tracing the transgressive surface and differentiating it from the seafloor throughout the seismic grid (Hogarth et al., 2007). A nominal velocity of 1500 m/s was used to convert travel time to sediment thickness. In order to convert travel time to sediment thickness, a velocity of 1720 m/s was used for non-silty sediments and a velocity of 1520 m/s was used for water and mud-dominated

sediments (Jackson et al., 1996; Williams et al., 2002; Buckingham & Richardson, 2002).The bathymetrical data used in this paper was acquired, processed, archived and distributed by the Seafloor Mapping Lab of California. We used the software Fledermaus by Interactive Visualization Systems (IVS 3D, http://www.ivs3d.com) to merge all graphic elements into three-dimensional perspective views of the seafloor and sub-bottom.

# Results

## Geology and Sediments

The CHIRP seismic profiles exhibit three distinct sedimentary packages or subunits (Figure 3):

1) The transgressive surface

2) Basal lag deposits

3) Modern Holocene deposits.

The transgressive surface, displayed in Figure 3, is identified by its pronounced truncation formed by wave-based and subaerial erosive processes. This erosion and truncation is thought to have occurred during multiple Pleistocene sea level lowstands and sea level transgressions (Hogarth et al., 2007).

The upper most unit observed in CHIRP seismic profiles displayed in Figure 3 is nearly transparent and displays both along-shelf and cross-shelf thickness variability, with a mid-shelf depocenter due to the transpressional and extensional forces which dictates sediment allocation. This seismically transparent uppermost unit comprises a majority of the sediment that overlays the transgressive surface (Hogarth et al., 2007). The modern Holocene upper unit is fine, to very fine-grained, homogenous sands based on cores acquired in the area (Darigo & Osbourne, 1986; Hogarth et al., 2007). Holocene sediment thickness decreases from approximately 10 m north of Scripps Canyon, to 0 m offshore Torrey Pines State Park (Hogarth et al., 2007; Le Dantec et al., 2010).

Perpendicular to shore, sediment thickness ranges from 0–5 m nearshore, to a maximum thickness of 10–20 m, in the mid-shelf region before thinning again as water depth increases (Hogarth et al., 2007). This systematic thinning observed in Figure 3, both along and across strike, leads to a wedge-shaped cross shore profile with a mid-shelf depocenter (Byrd et al., 1975; Henry, 1976; Hogarth et al., 2007). These well sorted, uniform modern marine Holocene deposits do not appear to have any lateral or horizontal reflectors as it is a uniform, well sorted, modern marine deposit (Rentz, 2010). There is a clear transition between the transgressive surface and the modern Holocene deposits, however the boundary between the basal lag deposits and modern Holocene deposits displayed in Figure 3 are less defined in the mid- shelf to outer-shelf region (Rentz, 2010; Le Dantec et al., 2010).

On the mid to outer-shelf region the transgressive surface is overlain by a poorly laminated basal lag deposit that is thought to have recorded the most recent Pleistocene sea level transgression (Le Dantec et al., 2010; Rentz, 2010). During sea level transgression wave-induced water motion erodes the highs and fills in both the lows and wave-cut notches that were formed by still stands and the falling limb of sea level (Rentz, 2010). Erosion of the highs occurs during sea level rises, the abrasion platform formed by wave orbital interaction with the sea floor shoals, leading to erosion of the coarser nearshore deposits and placing them over the fine-grained mid-shelf deposits (Rentz, 2010). The thickness of this basal lag deposit varies in accordance with the relief associated with the transgressive surface (Rentz, 2010).

In the northern part of the survey area, offshore Torrey Pines State Reserve, very little modern sediment deposition occurs 40-70 m depth as the mid-shelf thickness high is deflected seaward due to the shoaling of the transgressive surface from deformation associated with oblique faulting (Le Dantec et al., 2010). Because of the healing-phase of sea level transgression infill and reduced relief across the transgressive in the 70-120 m depth range, minimal thickness variation in the overlying transparent package is observed (Le Dantec et al., 2010).

**MCA Results**

A multiple correspondence analysis (MCA) allows us to analyze the frequency of distribution of surficial substrate composition, relative grain size, bedform structure, and relative slope of habitats along each ROV transect. The 14 variables used in this MCA analysis are displayed in Table 3.

A MCA was performed on the pooled data from all three ROV transect track lines corresponding to CHIRP lines 3, 5, and 7. Initial observations from each transect were used as an origin so that both distances from the origin and distances between distinct transitional boundaries substrates could be determined. The MCA results of all the pooled substrate are:

1). The first dimension of the MCA (MCA 1) accounts for 25.37% of the variance observed in the physical habitat substrate variability with a 0.761 positive correlation. MCA 1 was strongly correlated to habitat variables 4 and 14. Variable 4 displays loading coefficient with the most positive, strongest correlation, which scored 0.0187 representing a soft sedimentary habitat. Variables 4 and 14 represent soft sedimentary

habitats that are smooth, thereby lacking definitive bedforms. MCA 1 shows a lesser positive correlation with variables 9, 11, and 12 which score roughly 0.015 (Figure 4). These variables represent soft sedimentary muddy habitats that possess hatched or linguloid ripples as their diagnostic bedform. MCA 1 loading coefficients that score -0.00817 present a correlation with sloping boulder outcrops that lack sediment all together.

CHIRP 3 MCA 1 loading coefficients from the ROV video transects scored very positively due to the pervasiveness of soft sedimentary sands that lack distinct bedforms apart from being marked by bioturbation (Figure 5). This demonstrates the paucity of spatial coverage of outcropping transgressive surfaces or indurated dipping bedforms as the exposure of these surfaces is precluded by muddy sediments. The -0.013 scoring loading coefficient along CHIRP 3 occur at a depth of 67.9 m where we observe a 153 m long expanse of a mixture of boulder outcrops with fine-grained interstitial sediments. The -0.013 loading coefficient observed on CHIRP 3 along MCA 1 correspond to the transition from fine-grained Holocene sediments to lithified transgressive outcrop which occurs at 67.9 m depth.

Negative component loading scores of -0.013 along MCA 1were observed more frequently along CHIRP 5 and CHIRP 7 video transects which indicates a higher prevalence of sloping outcropping lithified habitats. Along CHIRP 5 the majority of lithified outcropping regions occur between 49.2-52.9 m, 70.5-71.8 m, and 85.1-93.3 m depth. On CHIRP 5 the most negative loading coefficient of -0.0085 occurred at 49.2 m

water depth corresponding to the transition from mobile Holocene sediments to lithified transgressive surface outcrops.

Along CHIRP 7 -0.013 loading scores along MCA 1 are observed between 45.7-68.4 m and between 88.2-93 m after which ROV became temporarily stuck on derelict fishing gear, as a result, the sampling transect was ended. The first negative loading coefficient, -0.013, at 45.7 m depth along CHIRP 7 is representative of the transition from modern Holocene sediment to outcropping lithified transgressive surface, which demonstrates the shoaling of the transgressive surface outcrops along strike.

MCA 1 density plots for all three CHIRP video transects were plotted demonstrating that CHIRP 3 is comprised almost entirely of soft sedimentary habitat with only a very small portion of the transect scoring ~ -0.02, delineating outcropping transgressive surface from 68.3-72 m depth (Figure 6). CHIRP 5 and CHIRP 7 display a negatively skewed distribution along MCA 1 demonstrating the higher proportion of sloping boulder habitats. Video transects corresponding to CHIRP 7 exhibit the most negatively skewed distribution. CHIRP 7 displayed a high density of negative values revealing that CHIRP 7 displays the greatest percent composition of sloping boulder habitats in comparison to modern Holocene sediments or basal lag deposits. The most negative -0.047 loading coefficients on CHIRP 7 are located at 90 m depth, where we observe a 10 m high boulder outcrop, which corresponds to the scarp offset induced by the RCF segmentation.

2). The second dimension, MCA 2, accounted for an additional 20.6% of the variability with a .617 positive correlation accounting for a combined 45.9% of the

observed variability within the first three dimensions of the data set (Figure 7). MCA 2 presented a positive correlation with variables 1, 6, and 10 which represent sloping boulder “habitats” that lack sediment all together. Sloping habitats, variable 6 displayed the most positive correlation along MCA. MCA 2 presented a negative correlation with variables 2 and 3, which represent a composition of rocks with sand and a sediment veneer habitats respectively. As in MCA 1, CHIRP 3 displayed a paucity of sediment veneer habitat, rocks with sand patches, and boulders except for a 153 m long expanse of boulder outcrops and sediment veneer habitat between the depths of 68.3-72 m. CHIRP 5 and CHIRP 7 displayed increased coverage of sediment veneer and rocks with sand habitats, as well as more variability in the flat sedimentary habitats, leading to very heterogeneous benthic environment (Figure 8). The location of the sloping boulder habitats corresponded to the negative loading coefficients as described in MCA 1.

The MCA 2 density plot demonstrates that CHIRP 3 is negatively skewed whereas CHIRP 5 and CHIRP 7 are positively right skewed. CHIRP 7 displays the greatest positively skewed distribution demonstrating its abundance of a variety of exposed rocky habitats which contain either coarse-grained interstitial sediments or lack sediment altogether (Figure 9).

3). The third dimension of MCA analysis, MCA 3, accounted for an additional 18.6% of observed variability giving a cumulative 64.6% of the total observed variability (Figure 10). MCA 3 presents a positive correlation with variables 2 (0.071), 7 (0.0159), and 9 (0.0388), representing a rock with sand composition with either coarse or muddy

sediments. MCA 3 loading coefficient scores of -0.0767 present a positive correlation with sediments with either linguloid or hatched ripples.

Along MCA 3, CHIRP 3 displays a distinct transition from -0.003 loading coefficients which represent a region of soft, flat, fine, and smooth sediments to a thin sediment veneer exposing lithified transgressive outcrops at 67.9 m which score (Figure 11). The transgressive surface outcrop observed at 67.9 m extends for roughly 153 m, which is followed by 0.0103 scoring loading coefficients representative of another transition from lithified transgressive surface outcrops to soft, flat, smooth, muddy sediments. This transition represented the shift from fine nearshore mobile sands to a muddier finer-grained offshore region of the shelf immediately following transgressive surface outcrops.

Video data from CHIRP 5 displayed a 576 m long expanse of hatched rippled fine-grained sediments that started from the origin at 40.9 m water depth and proceeded to 49.5 m depth. At 49.5 m depth we begin to see slight exposure of the transgressive surface under a fine-grained sediment veneer which progressed to full exposure of the transgressive surface boulder outcrops at 50 m depth. At a 56 m depth we observed an 862 m long expanse of soft, flat, fine-grained, hatched ripple sediment which occurred until a depth of 70.5 m. At 70.5 m we encountered a patch of boulders, rocks with sand, and sediment veneer habitats whose loading coefficients score 0.0155. This 34 m long patch of exposed hardground was followed by a 258 m long expanse of soft, flat fine-grained, hatched ripple sediments whose loading coefficients scored -0.024. At a depth of 77 m, the bedforms became less defined and very small to no sedimentary ripples were

observed for a 363 m linear expanse followed by a sediment veneer outcropping region at 85 m depth. This heterogeneous mix of outcrops, rocks with sand, and sediment veneers continued until 92.9 m where the sediments shifted to finer muddy sediment that persisted to a depth of 144.6 m where the transect was ended. The highest scoring loading coefficient, 0.0297, occurred at 92.9 m where we observed a rock with sand habitat that contained interstitial muddy sediments corresponding to variables 2 and 9, representative of MCA 3 habitat.

CHIRP 7 displayed the least variability in soft sedimentary habitats due to its prevalence of sloping boulder outcrops. CHIRP 7 MCA 3 loading coefficients scored moderately negative between -0.003 to -0.024 for the majority of the transect. Between the depths of 46.6-49.1 m a 173 m long expanse of 0.00046 loading coefficients were observed representing boulder fields which contained either coarse-grained or lacked sediments altogether. Soft, flat, fine-grained, smooth sediments reappear at 68.4 m for an 860 m expanse. A positive 0.0061 loading coefficient was observed at a depth of 89 m corresponding to the thin veneer of coarse sediments that overlay boulder outcrops on the seaward side of the fault scarp. At 93 m depth the ROV become entangled in derelict fishing gear and the survey transect was terminated.

The MCA 3 density plot suggests that CHIRP 5 exhibits the greatest variability in bedforms as it spans the entire bandwidth spectrum, and is not dominated by any one distinct feature (Figure 12). Bedform variability decreased both to the south to CHIRP 3 and to the north along CHIRP 7. CHIRP 3 and CHIRP 5 also exhibited a greater percent cover of very fine-grained muddy sediments that persisted from 72-101.6 m depth on the

CHIRP 3 and from 92-140 m depth on CHIRP 5. The CHIRP 3 transect displays two peaks along MCA 3 density plot that correspond to soft, flat, fine-grained, smooth sediments that scored -0.003, and soft, flat, smooth, muddy sediments which scored 0.01. CHIRP 5 displays these same two peaks in the MCA 3 density plot, however the percent cover of soft, flat, smooth, muddy habitat was not as pervasive as along CHIRP 3. CHIRP 5 exhibits a small peak at -0.0239 which represents hatched ripple sediments. CHIRP 7 exhibits a sharp peak at -0.003 representing the dominance of soft, flat, fine-grained, and smooth habitats as well as another sharp peak, which score 0.0046, representing soft, flat, coarse-grained, smooth sediments, whereas the other two transects lack coarse-grained sediment altogether. CHIRP 7 also displayed two less distinct peaks at 0.004-0.006 on the bandwidth spectrum which are lacking along the other two transects and represented the coarse sediments on the leeward side of the fault scarp, which are lacking along the other two transects.

4). The fourth and final dimension, MCA 4, accounted for an additional 17.4% of the variability within the data giving a final cumulative variance of 81.9% (for MCA's 1-4) (Figure 13). MCA 4 presented a positive correlation with variables 2 (0.106), 6 (0.025), 11 (0.037) and 12 (0.037) which represent sloping rock with sand habitats that have either hatched or linguloid ripples. MCA 4 also presents a negative correlation with habitats that have coarse grains and whose loading coefficients score -0.0932.

The CHIRP 3 video transect displayed loading coefficient scores of approximately 0 for the entirety of the transect along MCA 4. The positively scoring loading coefficients, 0.0297, along CHIRP 5 are attributed to the rocks with sand

habitats, while component loading scores of 0.0102 represent expanses of hatched ripple sedimentary bedforms. The remainder of CHIRP 3 scored close to 0 as this transect lacked the presence of coarse-grained sediments entirely (Figure 14). CHIRP 7 lacked any highly positive loading coefficients along MCA 4 as there were only sparse areas of rock with sand and no defined bedforms among any of the habitats. The two habitats that scored positively along CHIRP 7 correspond to sloping boulder outcrops that lack interstitial sediment (0.00678), and sloping, boulder outcrops with fine-grained interstitial sediments (0.00047) which both displayed sharp peaks in the MCA 4 density plot (Figure 15). Negative values that correspond to the coarse sediment as described in MCA 3 scored (-0.02559) when present in soft, flat, fine-grained sedimentary environments, and (-0.0257) when coarse-grained sediment veneers occurred on the seaward side of the fault scarp on CHIRP 7. CHIRP 3 and CHIRP 5 video transects lacked coarse sediment altogether, whereas CHIRP 7 displayed a presence of coarse sediment from 46-48.5 m as well as at 90 m depth on the seaward side of the fault scarp. The CHIRP 5 transect exhibited the greatest variability in sedimentary bedforms which predominate between 61.1-84.6 m depth.

In a secondary analysis habitats were grouped into clusters based on k-medoids as explained in the methods section. The 7 clusters presented in Table 4 best separated the data into distinct assemblages. After pooling all of the data to determine the unique habitat clusters, histograms were created displaying the percent composition of the seven unique clusters along each of the three ROV transects as a function of depth. (Figure 16)

Table 4: Seven unique habitat clusters obtained through k-medoids

| Cluster | CHIRP Line | Time | Comp. | Relative Angle | Grain Size | Bedform | Depth |
|---|---|---|---|---|---|---|---|
| 1 | 7 | 12:38:14 | Soft | Flat | Fine | Smooth | 91.7 |
| 2 | 5 | 13:48:23 | Soft | Flat | Mud | Smooth | 140.1 |
| 3 | 7 | 12:30:28 | Sediment Veneer | Flat | Fine | Outcrop | 88.6 |
| 4 | 7 | 11:04:38 | Boulder | Flat | Fine | Outcrop | 59.0 |
| 5 | 5 | 12:47:24 | Soft | Flat | Fine | Hatched Ripples | 91.3 |
| 6 | 7 | 12:43:01 | Boulder | Flat | None | Outcrop | 81.7 |
| 7 | 5 | 13:09:40 | Rocks with Sand | Flat | Mud | Outcrop | 93.3 |

The habitat composition of CHIRP 3 is dominated by clusters 1 and 2 with minor components of habitat clusters 3 and 4, supporting our results from MCA 1, in which fine and muddy sediments predominate along this southerly transect. Habitat clusters 1 and 2 are representative of soft, flat, fine-grained, and smooth as well as soft, flat, muddy, smooth habitats respectively (Figure 17). CHIRP 3 lacked habitat clusters 5, 6, and 7 and displayed minimal coverage of habitat clusters 3 and 4. Clusters 3, 4, 6, and 7 are all representative of outcropping environments that are impacted by local tectonic deformation which affects the relief of the transgressive surface, which in turn controls sediment bypass and accumulation (Le Dantec et al., 2010).

CHIRP 5 exhibits a component of each cluster type displaying pronounced habitat heterogeneity and substrate variability. CHIRP 5 is dominated by clusters 1, 2, 3, and 5 (Figure 17). Boulders, both with and without sediment, clusters 4 and 6, made up a small portion of total habitat along CHIRP 5. Along CHIRP 5 soft, flat, fine-grained,

hatched ripple sediments, represented by cluster 5, dominated between the depths of 40-49.7 m and 71-77 m depth. The cluster 5 patches are separated by interspersed sediment veneer patches and low relief boulder outcrops, clusters 3 and 4. These hatched ripple bedforms have a wavelength < 10 cm and are not observed on either CHIRP 3 or CHIRP 7 video transects. Less organized bedforms were observed at 89.5 m depth on CHIRP 5 which we have termed linguloid ripples. Due to the lack of occurrence of these linguloid ripples the cluster analysis did not isolate them as a distinct habitat. The very fine-grained muddy sediments, cluster 2, began to appear at 92 m depth and persisted to the shelf break. As described above, habitats 3, 4, 6, and 7 are representative of environments that are impacted by local tectonic deformation or past oceanographic processes, and therefore have some degree of hardground exposure. Cluster 3 habitats made up a substantial portion of hardgrounds along CHIRP 5. Sediment veneer habitats, cluster 3, exhibit the least amount of vertical relief of all hardground habitat clusters, 3, 4, 6, and 7. Habitat clusters 4, 6, and 7 represent the minority of habitats along CHIRP 5. Clusters 4, 6, and 7 exhibit greater vertical relief of transgressive surfaces than cluster 3 sediment veneer habitats. Cluster 3 habitats often lack surficial exposure of hardgrounds, and are only identified by the protrusion of sessile filter feeding gorgonians.

CHIRP 7 exhibited intermediate levels of habitat heterogeneity yet it exhibited the greatest habitat patchiness in comparison to the other two CHIRP transects (Figure 18). The dominant habitat clusters observed along CHIRP 7 included clusters 1, 3, 4, and 6 (Figure 17) Habitat cluster 1, persisted from 27-46 m depth. At 46 m depth, cluster 1 transitioned to habitat cluster 3 and 4 between the depths of 46-62 m, corresponding to

the transition from modern Holocene sediments to transgressive surface outcrops. There was then a 396 m long expanse of soft, flat, fine-grained sediments that persisted from 62-88 m depth. At 88 m depth a thin sediment veneer was observed until 89 m depth at which point we encountered a 10 m high outcrop of boulders that displayed 10 m of vertical relief. This fault scarp initially represented habitat clusters 3 and 4 and then transitioned to habitat cluster 6 directly over the fault scarp which was devoid of sediments. This outcrop lines up with the fault scarp observed in both the sub-bottom profiling data as well as the multibeam swath bathymetry. After descending the seaward side of the fault scarp, we entered an expanse of thin coarse-grained sediment veneer habitat with abundant shell hash, which due to its limited coverage is not expressed in any of the seven habitat clusters.

CHIRP 3 exhibited the least habitat fragmentation and therefore the greatest average distance between sedimentary and hardground habitat patches followed by CHIRP 5 and then CHIRP 7. The large spatial coverage of sedimentary patches is due to the thickness of nearshore sediments which extend offshore until 68.3 m thereby limiting exposure of transgressive surface outcrops and dipping Pleistocene bedforms. Moving north, along strike, habitat heterogeneity increased inversely to patch length as the transgressive surface exposure shoaled and sediment thickness decreased causing increased habitat fragmentation and patchiness (Figure 18).

When the density distribution of clusters 1-7 in the pooled data of all three CHIRP transects was analyzed as a function of depth, we observed that the most dominant habitat cluster in the nearshore was cluster 1, representing flat fine-grained sedimentary habitat

(Figure 19). Cluster 2 was the most dominant of the outer-shelf habitat types and was observed on the seaward side of the pop-up structure. Habitat clusters 3-7 were observed primarily along the mid-shelf region between 40-90 m which was where we observed the most habitat heterogeneity. This demonstrates that soft, flat, fine-grained sedimentary habitats comprised the majority of available substrate along all transects except in regions where sub-bottom profiling displayed the shoaling of the transgressive surface or the presence of dipping Pleistocene bedforms deposited through retrograde deposition.

A boxplot of cluster habitats as a function of depth showed that habitat cluster 1 covered the greatest spatial area from 25 to 100 m depth (Figure 19). In general, this smooth, flat, fine-grained sedimentary habitat, cluster 1, transitioned to a smooth, flat, finer-grained, muddy habitat, cluster 2, at approximately 75 m depth on the seaward side of the transgressive surface outcrops. The outcropping boulder habitats, clusters 4 and 6, are limited to a range of 50-85 m water depth corresponding to the areas of most tectonic deformation. Hatched ripple sedimentary habitat, cluster 5, was only observed along CHIRP 5 and correspond to roughly the same depths as exposed transgressive surface outcrops. Cluster 3 habitats represent the thinning of mobile sands on the landward and seaward sides of exposed transgressive surface outcrops and within indurated dipping Pleistocene bedform habitats.

The cluster 4 density analysis as a function of depth along CHIRP 3 displayed peaks at 65 and 75 m demonstrating that boulder outcrops along CHIRP 3 are localized to very small areas in comparison to CHIRP 5 and CHIRP 7 due to minimal tectonic deformation and transpressional uplift (Figure 20). CHIRP 5 exhibits two smooth peaks

at 45 m and 75-80 m. The peak at 45 m is representative of outcropping transgressive surface while the smaller peak from75-80 m depth is representative of indurated dipping Pleistocene sediments formed through retrograde sediment deposition during asymmetric sea level fall (Hogarth et al., 2007; Le Dantec et al., 2010). CHIRP 7 displayed peaks at 45m, 55 m, and 65 m which represent uplifted transgressive boulders with interstitial fine-grained sediments.

CHIRP 5 was the only transect that displayed peaks in the cluster 5 density plot as a function of depth (Figure 21). Hatched ripple sediments occurred from 35- 50 m water depth and declined leading up to the outcropping transgressive surface. The CHIRP 5 ROV survey began at 35 m, so it cannot be said with certainty that these hatched ripple bedforms did not persist to the shore. Cluster 5 was also observed on the seaward side of the transgressive surface outcrops at 60 m which steadily declined after 70 m depth. In deeper, lower energy environments, habitat cluster 5 was replaced by muddy and sediment veneer environments.

CHIRP 5 and CHIRP 7 cluster 6 density analyses as a function of depth both displayed peaks at 50 m and 80 m. The peaks observed at 50 m and 80 m along CHIRP 5 and CHIRP 7 displayed differing amplitudes among transects. This demonstrates that there is greater proportion of boulder outcrops without sediment on CHIRP 5 at 50 m and a greater proportion of boulder habitats without sediment on CHIRP 7 at 80 m. (Figure 22) Cluster 7 habitats were only observed along CHIRP 5 at 75 m and 95 m, as this transect displayed interstitial fine-grained muddy sediments within exposed hardgrounds.

**Biological Results**

A list of all the biological organisms identified is listed in Table A-1.The RDA on the explanatory and response variables returned four dimensions of eigenvalues whose values are presented in Table 5. The first two dimensions of eigenvalues, RDA 1 and RDA 2, account for a majority of the variance in the constrained analysis of biological species data. Using the organismal eigenvalues from RDA 1 and RDA 2, species were grouped based on correaltions with one or more of the four MCA habitat RDA 1 and RDA 2 eigen values displayed in Table 5.

Table 5. Constrained across all four dimensions of redundancy analysis of nominal categorical physical data constraining organismal data counts.

| Components | RDA 1 | RDA 2 | RDA 3 | RDA 4 |
|---|---|---|---|---|
| Constrained Eigen Values | .6892 | .2827 | .2365 | .1960 |

Figure 24 displays a biplot of both site and variable eigenvalues from RDA 1 and RDA 2 depicting both observed and predicted species habitat correlations. Organisms whose eigen values scored positively along RDA 1 and RDA 2, exhibit a correlation with MCA 2 hardground habitat. Schooling fish demonstrated the correlation with MCA 2 habitats and were found in high densities along CHIRP 5 and CHIRP 7 which displayed increased spatial coverage of MCA 2 harground habitats.

Organisms whose eigen values scored positively along RDA 1 and negatively along RDA 2 displayed associations with both MCA 2 and MCA 3 habitats. All sessile

suspension feeding gorgonians, cup corals, tunicates, and sponges were included in this grouping. *Parazoanthus lucificum* (An), *Adelogorgia phyllosclera* (Ap), *Eugorgia rubens* (Eu), *and Leptogorgia chilensis* (Lo) were all included in this MCA 2/MCA 3 grouping and were summed across individual CHIRP transect video snippets to observe differences in the presence of organismal numbers between transects. Each of the four species observed in individual video snippets were summed throughout the entirety of each individual transect as shown in Table 6.

Table 6. Summation of gorgonians and zoanthids across individual transects.

| CHIRP Line | *Parazoanthus lucificum* (An) | *Adelogorgia Phyllosclera* (Ap) | *Eugorgia rubens* (Eu) | *Leptogorgia chilensis* (Lo) |
|---|---|---|---|---|
| 3 | 28 | 312 | 14 | 22 |
| 5 | 29 | 638 | 10 | 46 |
| 7 | 20 | 463 | 84 | 216 |

All three gorgonian species, *Adelogorgia phyllosclera, Leptogorgia chilensis, and Eugorgia rubens* displayed increasing numbers as we move north from CHIRP 3 to CHIRP 7. This demonstrates that the number organisms whose RDA 1 and RDA 2 eigenvalues correlate with MCA 2 habitats increased in accordance with the increasing spatial coverage of MCA 2 habitat. Along CHIRP 3 *A. phyllosclera, L. chilensis, and E. rubens* were observed from 67.3-71.1 m where transgressive surface hardgrounds outcroped. Along CHIRP 5 we observed gorgonians at 45-52 m, 70-72 m, and 85-96 m depth. CHIRP 7 displayed a similar pattern in which gorgonians were observed from 45-

54 m, 59-62m, 68m, and 87-93 m depth. The presence of gorgonians at depths greater than 55 m is attributed to the exposed dipping Pleistocene sediments deposited during asymetric sea level regression. The induration of these east-west dipping sediments is demonstrated by their displayed relief in CHIRP seismic profiles and exposed hardgrounds in ROV video data which create vertical relief on the seafloor and habiatat for sessile suspension feeders. The distribution of gorgonians mirrors the presence of hardgrounds exposed through past tectonic and oceanopgraphic processes.

Organisms whose eigenvalues scored negatively along both RDA 1 and RDA 2 axes displayed associations with MCA 3 habitats, rocks with interstitial coarse-grains or mud. MCA 3 habitats were observed on the periphery of exposed transgressive surface outcrops, as well as along the dipping Pleistocene sediments on ther outer shelf between 75 and 85 m depth . The crinoid, *Florometra serratissima,* was oberved in these MCA 3, rock with sand and sediment veneer habitats on  both CHIRP 5 from 92-96 m and on CHIRP 7 at 50 m.

Organisms that were observed along the perimeter of two distinctly contrasting habitats diplayed  pronounced edge effects most notably in their occupancy, motility, and foraging patterns. Areas that displayed increased habitat fragmentation exhibited pronounced edge effects. By residing on the edge of different habitats these organisms create functional changes in ecological processes and trophic dyanmics of complex food webs (Valladares et al., 2006). *Rhinogobiops nicholsii,* blackeyed gobies, do not present a strong correaltion with any one habitat, demonstrating an edge effect due to their foraging practices. *R. nicholsii* were often observed along the periphery of boulder patches and in

the proximity of smaller scale rock with sand habitats. In conjunction with *R. nicholsii*, the *Acanthoptilum spp.* of sea pen displayed an association with MCA 3 habitat and to a smaller extent MCA 2 habitat. *Acanthoptilum spp.* were often observed amid the patches of coarse-grained sediment that occurred on the edges of boulder patches where sediments thickened.

*Lytechinus anamesus*, white urchin, displayed a broad range of habitat associations and were observed along all three CHIRP transects. *L. anamesus* displayed loose correaltions with MCA 3 habitat and to a smaller extent MCA 1 habitat. Along CHIRP 5 approximately 256 individual *L. anamesus* were observed per 5-second video segment within outcrops that occurred at 72 m as well as in the sediment veneer habitats between 90-96 m depth. A similar pattern occurred along CHIRP 7 where we observed *L. anamesus* at 45 m, 60 m, and 90 m depth within sediment veneer habitats that accomodate sessile suspension feeders and schooling fish. *L. anamesus* were not limited to MCA 3 habitat, however, their highest densities coincided with sediment veneer and slightly rocky habitats. *L. anamesus* and infaunal ophiuroids were the most pervasive of the benthic suspension/deposit feeders. As evidenced from the RDA however, *L. anamesus* were observed more frequently in coarse and muddy rocks with sand MCA 3 habitats, while infaunal ophiuroids were associated with fine grained sedeimentary MCA 1 habitat.

Infaunal suspension feeders, mobile predators such as *Mitra idae*, and sediment associated asteroids eigenvalues were correlated with MCA 1 and MCA 4 habitat**.** Infaunal ophiuroids and infaunal polychates, *Diopatra spp.*, were the predominate

organisms in nearshore and offshore MCA 1 sedimentary habitats. Infaunal ophiuroid eigenvalues along CHIRP 5 scored closely with MCA 1 and MCA 4 eigenvalues, due to their occurrence in smooth sediments and rocks with either hatched or linguloid sedimentary bedforms. Along CHIRP 7 infaunal ophiuroids were the predominat organim in MCA 1 habitat. *Astropecten spp.* were observed in the nearshore sedimentary environment however they were replaced by *Luidia foliolata* in the muddier offshore habitats from 60-120 m depth. Lizard fish, *Synodus lucioceps*, were very prevalent in the nearshore soft, flat, fine-grained sedimentary environments. Octopus and octopus dens were observed in the fine-grained and finer-grained muddy sediments of MCA 1 habitats which lacked bedforms. These octopus dens occurred in a soft, often muddy, sedimentary environment marked by heavy bioturbation. Because our ROV surveys were performed during the day there was not sufficient data to draw conclusions on octopus distributions and habitat associations of other nocturnal organisms.

The RDA biplot from the pooled data analysis gives a coarse resolution of organismal asociations with habitats because it is based on an average of species habitat associations along all CHIRP transects. In order to obtain a finer scale resolution of organismal habitat associations along individual CHIRP transects the data matrix was analyzed individually for each CHIRP line, and an RDA biplot was produced for each transect.

CHIRP 3 MCA scores and biological count data were subsetted from the pooled data and analyzed with a RDA. Figure 25, created from the CHIRP 3 RDA, displays both lower species richness and subordinate species correaltions with MCA 2 boulder habitat.

Gorgonians, sponges, and cup corals whose eigenvalues were associated with MCA 2 and MCA 3 habitats in the pooled RDA, display looser correaltions in the CHIRP 3 RDA biplot.

The CHIRP 5 RDA bilpot, Figure 26, displays a close resemblance to the biplot of the pooled data, Figure 24, most notably MCA 2 and MCA 3 habitat associated organisms. One observed difference is that *Lytechinus anamesus* scored more closely with MCA 4 habitat as opposed to MCA 1 or MCA 3 as they did in the pooled RDA. *Acanthoptilum spp*. eigenvalues demonstrate a correlation with MCA 1 and MCA 2 habitats along CHIRP 5, whereas in the pooled biplot *Acanthoptilum spp.* eigenvalues scored more closely with MCA 1 and MCA 3 habitats.

The RDA biplot for CHIRP 7 displays tight correlations and similar species patterns to the biplot from the pooled data RDA, Figure 27. The length and magnitude of the species vectors assocaited with MCA 2 sites along CHIRP 7 are longer than either CHIRP 3 or CHIRP 5 biplots, demonstrating higher species abundances associated with MCA 2 and MCA 3 habitats. The angles between CHIRP 7 species vectors and the MCA 2 habitat are less than both CHIRP 3 and CHIRP 5 organismal vectors, implying greater positive correaltions.

Sessile suspension feeders have a tight association with the physical habitat and therefore their presence is highly indicative of hard substrate and increased ambient bottom flow. Cnidarians from all three CHIRP transects were analyzed using an RDA apart from other organisms. From this biplot we observed that *Eugorgia rubens and Leptogorgia chilensis* were tightly correlated to MCA 2 habitat whereas *Balanophyllia*

*elegans*, *Adelogorgia phyllosclera*, and *Parazoanthus lucificum* are display weaker correaltions with MCA 2 and MCA 3 habitats (Figure 28). The sea pens, *Acanthoptilum spp., Stylatula elongata, Virgularia mirabilis*, and the sand anemone *Phyllactis spp.* exhibited correaltions with both MCA 1 and MCA 3 habitats. Figure 28 demonstrates habitat partitioning amongst hard substrate requiring and sediment anchored sessile suspension feeding cnidarians.

Figure 29 displays RDA 1 and RDA 2 eigenvalues for the finfish analyzed using a RDA. *Chromis punctipinnus, Sebastes spp., Rhacochilus toxotes, and Semicossyphus pulcher* displayed a tight associationwith MCA 2 habitats and displayed greater abundances in the northerly CHIRP 5 and CHIRP 7 transects which exhibited increased presence of hardground exposure and habitat heterogeneity. These observations, depicted in Figure 30 reflect the classic species-area curve of MacArthur & Wilsons (1967) in their theory on island biogeography, which shows that larger spatial areas should exhibit greater species richness.

The other grouping of fish includes lizard fish, combfish, and flatfish, senoritas which all scored negatively along RDA 1 and are more closely correlated to the other three MCA (1-4) sites excluding MCA 2. Blackeyed gobies, *Rhinogobiops nicholsii,* appear to distinguish themselves among finfishes in that they do not express tight correlations with any of the above MCA habitats. As stated above, blackeyed gobies were often observed between boulder patches and along the edges of these boulder fields, demonstrating pronounced edge distributions. *R. nicholsii* edge effects relate to

occupancy and motility within the structural framework provided by boulder outcrops as well as for foraging within sedimentary environments on the periphery of outcrops.

Organisms presenting correlations with MCA 1 habitat do not display as discernable or robust of a trend as MCA 2 associated organisms. *Lytechinus anamesus* displayed a maximum numer of individuals in the sampled regions along CHIRP 5 and the lowest number of individuals along CHIRP 3. Based on these numbers *Lytechinus anamesus* appear to prefer a slightly higher current regime which reflects their association with MCA 3 habitat, and is also why their maximal values correspond to CHIRP 5. *L. anamesus* are a mobile species which may leads to the ephemerality of their distribution and therefore trends in their distribution cannot be deduced with certainty.

# Discussion

## Geological and Physical

Increased tectonic deformation from left jogs in the oblique right-lateral strike-slip RCF, has led to both the uplift and shoaling of the transgressive surface. The shoaling of the transgressive surface has led to diminished sediment thickness over the Torrey Pines pop-up structure leading to increased patchiness, hardground exposure, and habitat heterogeneity. The distribution of hardground associated sessile suspension feeders, such as gorgonians, corresponds to transgressive surface outcrops formed exposed through tectonic transpressional forces as well as indurated dipping Pleistocene bedforms deposited through retrograde deposition. Both the physical habitat heterogeneity and biological species richness increases in accordance with fault segmentation along the RCF which decreases sediment thickness and increases habitat fragmentation through the uplift of the transgressive surface.

CHIRP 3 lacks both bedforms and coarse sediment which is indicative of a low energy depositional environment. This low energy environment allows for fine-grained and finer-grained muddy sediments to settle out that under higher energy environments would be suspended and entrained in the water column. This low energy environment results in a smooth, soft, fine to very fine-grained sedimentary environment. Particle size and the velocity of the medium determine the type and wavelength of the resulting bedforms. Because CHIRP 3 exhibited fine-grained sediments lacking distinct bedforms, we propose that this is a depositional environment that lacks sufficient energy to keep fine grained particles in suspension. When velocity is decreased the competence, or size

of particles a defined flow is capable of transporting, is lowered and fine grained particles settle out and deposit on the seafloor. The minimal spatial coverage of transgressive surface outcrops along CHIRP 3 is due to the lack of relief along the transgressive surface which promotes sedimentary infilling rather than erosion. This lack of vertical relief can be attributed to the linearity of the dextral strike slip fault just north of the Scripps Canyon.

CHIRP 3, the most southerly transect, is representative of a low energy depositional environment, which lacks prominent outcropping transgressive surface faces, in comparison to the more northerly transects, CHIRP 5 and CHIRP 7, which are impacted by segmentation and step overs of RCF. This obliquity of the strike-slip component of the RCF creates transpressional uplift causing transgressive surface hardgrounds to outcrop which provide a unique structural framework for sessile suspension and filter feeders, as well as a diverse assemblage of fish species and detrital deposit feeders.

CHIRP 5 exhibited intermediate levels of patchiness and the greatest levels of habitat heterogeneity in comparison to CHIRP 3 and CHIRP 7. Although its average patch lengths are slightly longer than CHIRP 7, CHIRP 5 displayed the greatest substrate variability and heterogeneity as it includes all seven habitat clusters. CHIRP 5 displayed a balance between depositional and erosive processes and displays both thin veneers of sediment between boulder outcrops as well as hatched ripple sedimentary bedforms. These hatched ripple bedforms occur in the nearshore region and in between patches of boulder outcrops from 35-70 m depth. In deeper lower energy environments the fine-

grained, hatched ripple sediments are replaced by mud and sediment veneer habitats. The presence of all 7 habitat clusters along CHIRP 5 makes it the most diverse and heterogeneous transect in the survey. CHIRP 7 on the other hand did not display as much habitat heterogeneity however it displayed the most habitat fragmentation, patchiness, and therefore the greatest density of edge habitat.

Along CHIRP 7 the tectonic forces resulting from segmentation along the RCF have produced an erosive hydrographic environment with pervasive exposed boulder outcrops and reduced spatial coverage and thickness of modern Holocene sediments. CHIRP 7 exhibited the most patchiness between habitat types due to its location at the apex of the pop up structure which creates a heterogeneous environment with small scale localized patches of rocky environments and increased edge density. By understanding the size and composition of habitat patch structure we can defines ecological processes for many species, both mobile and slightly mobile.

**Biological Discussion**

As we moved along strike of the RCF we observed a significant increase in species richness along individual CHIRP lines clearly demonstrates increased species richness to the north, towards the apex of the pop-up structure, along strike of the RCF. CHIRP 3 contains the least species richness with 30 organismal groups in comparison to CHIRP 5 and CHIRP 7, which contain 45 and 54 organism groupings respectively (Figure 30). The organisms absent from CHIRP 3 include a variety of sponges, fishes, and tunicates. Many of these organisms display associations with MCA 2 and MCA 3 habitats in the pooled data RDA biplot. Increased species richness along CHIRP 5 and

CHIRP 7 can be attributed to underlying tectonic transpressional forces leading to increased habitat heterogeneity and biological specialization as well as bathymetrical features formed through past oceanographic processes.

Both CHIRP 5 and CHIRP 7 contain a greater spatial coverage of MCA 2, MCA 3, and MCA 4 habitats due to their proximity to the RCF transpressional pop-up structure. This increased spatial coverage of hardground habitats appears to have led to increased species diversity, supporting the niche theory as presented by Hutchinson (1957), MacArthur & Wilson (1963, 1967), and Silvertown (2004). The niche theory predicts a positive relationship between species richness and habitat heterogeneity through niche partitioning. Whittaker et al., (1973) and Legendre & Legendre (2012) state that one of the most important components of ecological community structure is environmental heterogeneity. It has been widely accepted that a heterogeneous environment provides more niches than uniform homogenous environment and is able to support more diverse communities (Legendre & Legendre 2012; Buhl-Mortensen et al., 2010). The rocky patch structure along CHIRP 5 and CHIRP 7 displays both greater spatial coverage and decreased isolation distance between patches leading to increased edge density and edge effects. The increased presence of isolated rocky patches impact not only hardground associated organisms but the species composition of surrounding sedimentary habitats due to foraging by organisms such as *Rhinogobiops nicholsii*. *R. nicholsii* utilize rocky outcrops for occupancy and mobility between environments, however they forage in adjacent sedimentary habitats, thereby changing the trophic dynamics of both habitats.

CHIRP 3 displays limited transgressive outcrops from 67-71 m depth. From 71-122 m depth CHIRP 3 displayed a rather homogenous, smooth, muddy, sedimentary environment with significant bioturbation and sparse shell hash. Not only does CHIRP 3 lack pronounced MCA 2 habitat, it also lacks organisms that displayed tight correlations with MCA 2 habitats in the pooled RDA biplot. The summation of the three gorgonian species, *Adelogorgia phyllosclera, Leptogorgia chilensis, and Eugorgia rubens* along individual CHIRP lines demonstrate reduced numbers of sessile suspension feeders along CHIRP 3 as well as looser correaltions between organismal vectors and MCA 2 sites.

Organisms whose biplot vectors express correlations with MCA 2 and MCA 3 habitats in the pooled data biplot demonstrated a much looser correlation in the CHIRP 3 biplot, Figure 25. MCA 2 and MCA 3 associated organisms along CHIRP 3 display greater angles between organismal vectors and MCA 2 and MCA 3 sites, inferring a loose correlation. CHIRP 3 hardground associated organisms display a stronger correlation with MCA 4 and MCA 3 habitats. Along CHIRP 5 and CHIRP 7 the hardground associated organisms relationship is tightly correlated with MCA 2 and MCA 3 habitats. The likely reason for the lack of tight correlations with MCA 2 habitat along CHIRP 3 is attributed to the lack of MCA 2 habitat which requires a stronger flow regime with higher bottom velocities induced by transpressional uplift through fault segmentation of the RCF. The uplifted transgressive surface within the Torrey Pines pop-up structure as well as the fault scarp observed along CHIRP 7 at 80 m depth act as alongshore ridges that appears to dam sediments from moving straight offshore and downslope, thereby exerting control of sediment allocation along the continental shelf.

CHIRP 5 displayed three extensive regions of outcropping at 50-52 m, 72 m, and 86-95 m depth, while CHIRP 7 displays outcrops from 45-55 m, 60 m, and 85-95 m depth. CHIRP 5 and CHIRP 7 therefore exhibit a great deal more patchiness and less habitat isolation between rocky outcrops. The rocky habitats CHIRP 5 and CHIRP 7 cover a greater spatial area and are more evenly distributed along the transect decreasing isolation distance between patches has led to a patchy mosaic of rocky habitats adjoining soft and hard bottom substrates. Patch structure plays an important role to mobile foraging species such as *L. anamesus* and epifaunal brittlestars due to increasing species richness, productivity and decreased isolation between patches. Patch structure influences mobile foraging species such as *L. anamesus* and epifaunal brittlestars by decreasing isolation between patches allowing for increased mobility. As isolation between patches decreases mobile predators should be able to cover a larger spatial area and pick over adjacent sedimentary habitats altering the trophic and community structure in comparison to larger more isolated patches. These findings are consistent with MacArthur and Wilson's (1963 & 1967) island biogeography theory which suggests that both the area and geographical isolation affect both colonization and extinction rates. This theory predicts that species richness will display a positive correlation with habitat patch, "island", size and a negative correlation with the degree of isolation. Our observations of increased species richness with increased spatial area of rocky habitats and reduced spatial isolation between patches supports an island biogeography model in this environment.

This decreased spatial coverage of MCA 2 habitat along CHIRP 3 greatly affects the angular correlations of species vectors with MCA 2 habitat in the RDA biplot. The majority of CHIRP 3 rocky habitats were classified as MCA 3 and MCA 4 as opposed to MCA 2. The increased spatial coverage of MCA 2 along CHIRP 5 and CHIRP 7 is the causal factor in tightening the correlation between hardground associated species vectors and MCA 2 habitats. The organism that displayed the tightest correlations to MCA 2 was schooling fish. The lack of schooling fish along CHIRP 3 was attributed to the lack of suitable MCA 2 habitat in which schooling fish were observed in high densities along CHIRP 5 and CHIRP 7. MCA 2 habitats lack interstitial and surrounding sediments and therefore provide a greater percent coverage of hard substrate over a given area in comparison to sediment veneer and rocks with sand habitats. Due to this increased spatial coverage of hardground we would expect greater recruitment and greater species richness of hardground associated organisms as predicted by the species area curve (MacArthur & Wilson, 1967). Increased species richness and finfish numbers may have trophic cascade effects directly resulting from habitat arrangements based on geological and oceanographic alteration of bathymetric contours and bottom currents.

CHIRP 3 displayed limited spatial coverage of MCA 3 habitats which were favorable for organisms such as *Florometra serratissima,* and *Lytechinus anamesus.* We propose that these MCA 3 habitats are more ephemeral than MCA 2 habitats, due to their low lying relief and presence of surrounding sediments that may scour the surface of rocks. These ephemeral MCA 3 habitats are therefore well suited for mobile opportunistic settlers, as there is less competition for space due to sediment scouring and

burial. Coarse-grained sediments within sediment veneer habitats demonstrates that these habitats experience increased bottom flow explaining the increased presence of mobile suspension feeders such as *Florometra serratissima*, and *Lytechinus anamesus.*

The fish RDA biplot demonstrates that *Chromis punctipinnus, Sebastes spp., Rhacochilus toxotes, and Semicossyphus pulcher* displays tight correlations with rocky MCA 2 habitats. We propose that these fish utilize shelter from boulders and secondary biogenic structures as well as benefitting from resuspension of particles due to the altered flow regime, associated with boulder habitats. The other group of finfishes listed in Table A-1 (lz, scom, lcom, se, and ch) were correlated with MCA 1 and MCA 3 habitats as opposed to MCA 2 habitat. *Rhinogobiops nicholsii* propensity for residing along the periphery of distinct habitats, edge effect, has led to a loose correlation with any one habitat. The elevated patchiness of CHIRP 5 and CHIRP 7 increases the area of edge habitats which would explain why *R. nicholsii* numbers dramatically increased from CHIRP 3 to CHIRP 7. This has secondary effects on trophic dynamics and structure of adjacent biological communities.

The reduction in species diversity along CHIRP 3 supports the hypotheses that this transect lacks pronounced heterogeneity of the sea floor and is dominated by flat, smooth, soft, sedimentary habitats with limited boulder and rock exposure. This would explain the decrease in hardground associated organisms observed along CHIRP 3. CHIRP 3 lacks breadth of hardground habitats leading us to expect there to be less species diversity and richness in comparison to the northerly transects. The larger spatial coverage of MCA 2, MCA 3, and MCA 4 habitats, which represent a variety of

hardground habitats,  along CHIRP 5 and CHIRP 7 leads to greater habitat heterogeneity hardground habitats and an increased number of species that are successful after immigration and settling. There are differential foraging effects as fish forage away from hardground habitat and affect the trophic and community structure in nearby sediment communities.

Soft sedimentary habitats were not as well sampled because they tended to cover larger spatial area yet still were analyzed with five, 5-second video snippets.  Therefore numbers of *Astropecten spp., Luidia spp., Stylatula elongata*, and infaunal ophiuroids are not as robust or reliable in determining the total number of individuals.

## Conclusion

In conclusion, the narrow continental shelf has modified through aerial exposure during low stand glacial periods, wave based erosion, wave cut notches, tectonic deformation, and present wave based and longshore erosional processes. The overprinting of these physical processes has led to a rich tapestry of physical settings, flow regimes, and heterogeneity of benthic habitats allowing for diverse partitioning of biological assemblages. The joint segmentation/jogs of the RCFZ have created components of transpressional and extensional areas that govern sediment bypass, deposition, and erosional processes that dictate biological utilization of habitats. Segmentation along the RCF and relief thereby controls sediment thickness and grain size as well as the proportion of consolidated transgressive surface outcrops. This partitioning has secondary effects including patch structure, species richness, habitat heterogeneity, and secondary trophic effects such as those created by edge effects.

Segmentation along the RCF has led to a dichotomy of habitats whose heterogeneity increases as we move along strike of the RCF towards the apex of the pop-up structure. Species numbers, species richness, and edge effects increased along strike as habitat heterogeneity, the spatial scales of rock outcrops, and bottom current flow increased concomitantly. Our observations are supported by island biogeography theory, species area curve, and niche theory as presented by MacArthur and Wilson (1967).

By increasing our understanding of the underlying tectonic processes and past and present oceanographic processes occurring on the continental shelf and its relationship to sedimentary and hardground habitat, we can better predict ecological processes and

species utilization of the habitats. This study provides baseline measurements and an understanding of the complex geological, hydrographic, sedimentary and biological interactions in the region. The exploration of this area to determine the ecology and occurrence of the soft corals is necessary to support the conservation and long-term protection of these coral populations along the San Diego shelf and continental shelves globally.

This study elucidates tectonics role in altering the local hydrographic regime through bathymetrical features and submarine canyons, which modify flow, internal waves, sediment and nutrient distribution. As tectonic deformation increases along strike it modulates bathymetrical features of the seafloor most notably the shoaling of the transgressive surface which impacts sedimentary processes leading to habitat partitioning and benthic habitat variability.

Habitat provisioning and patch structure are important components in understanding associations of organisms with their habitat, community structure, and trophic cascades. This study attempts to understand the modulation of ecological processes through tectonics and the scales at which these interactions occur. The implementation of CHIRP seismic data, multibeam swath bathymetry, and ROV ground truthing video data greatly increases both the surficial and subsurface spatial resolution of predicting ecological processes at the appropriate scale. The geophysical techniques and results of this study can be extrapolated to other areas to better understand ecological connections among continental shelf habitats and manage these areas for conservation and anthropogenic exploitation. As anthropogenic impacts become greater it is important

to understand the complex interactions of geology, biology, and ecosystem processes to mitigate degradation of the nearshore shelf environments.

## Figures

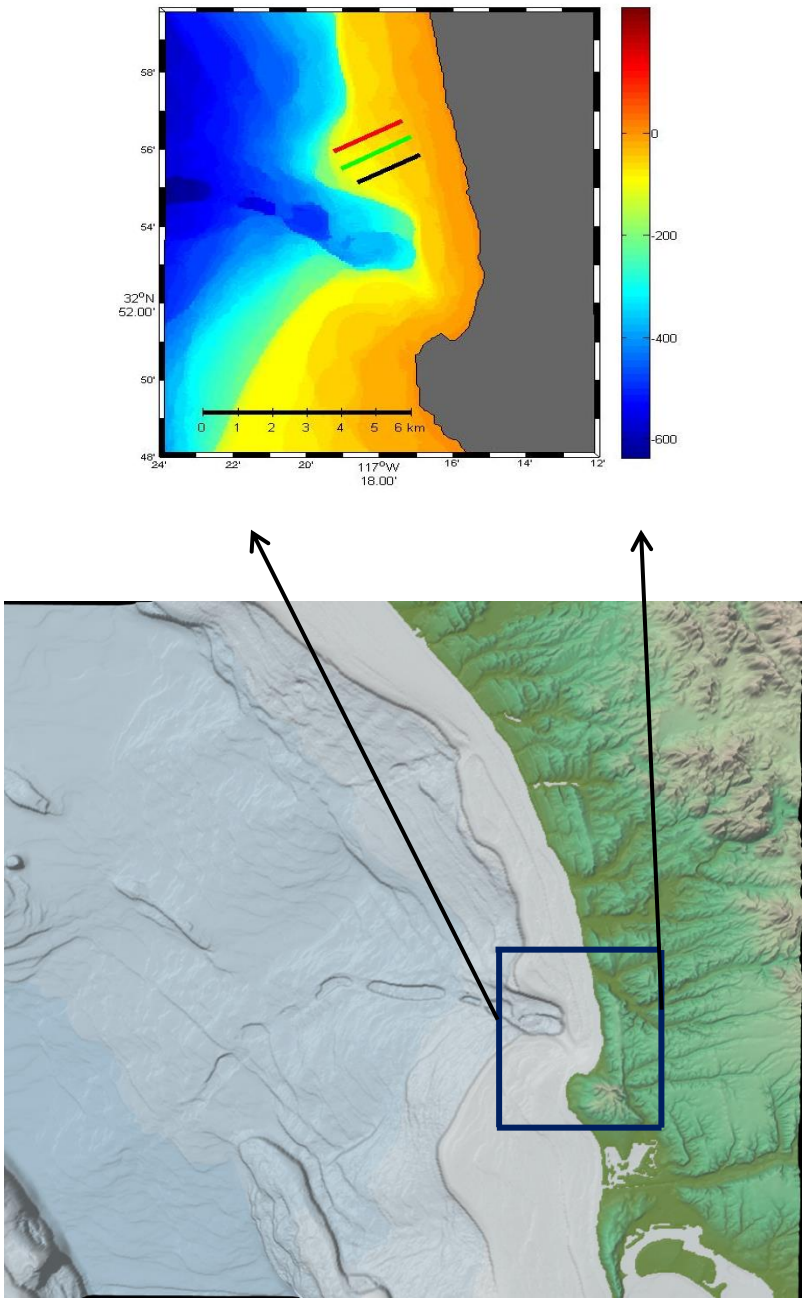


Figure 1. Map of La Jolla, Southern California. The location of the study area and the three transects are shown in the inset.

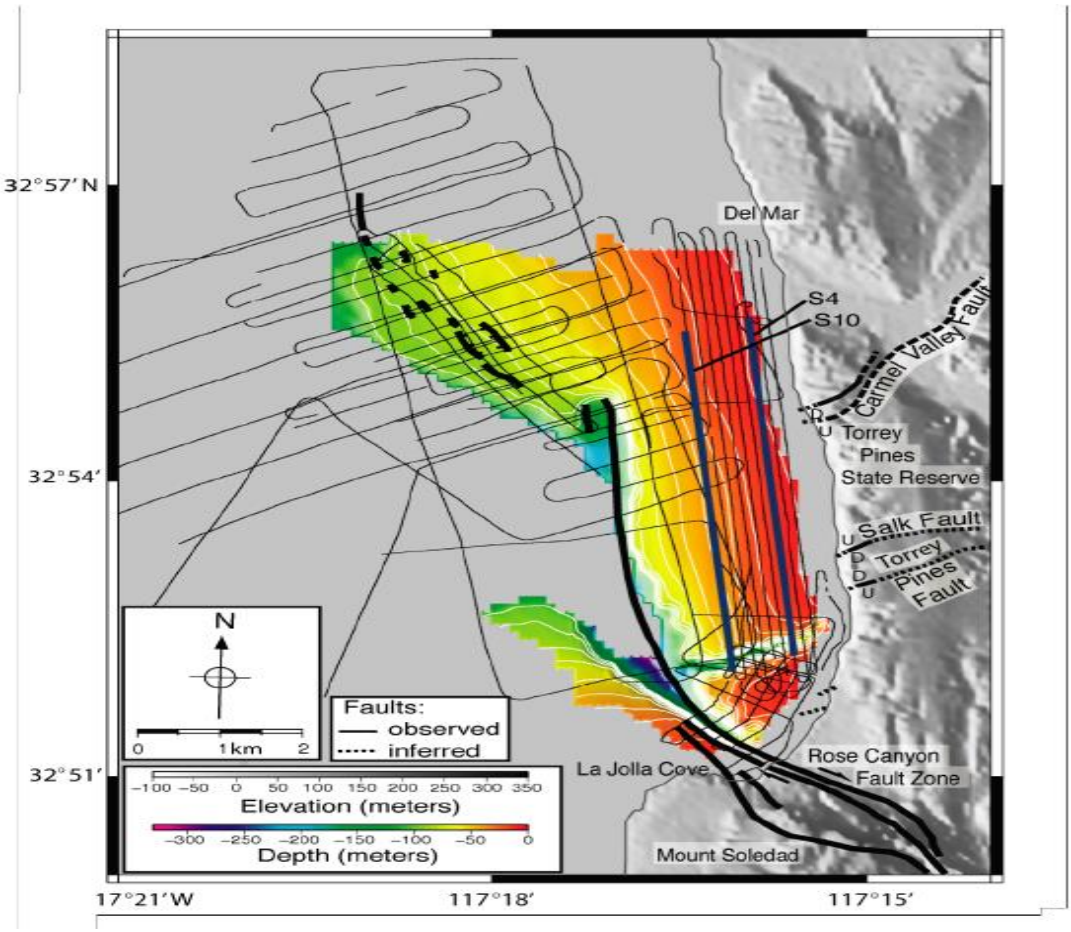


Figure 2. Map of survey area and CHIRP seismic transects characterizing the Rose Canyon Fault.

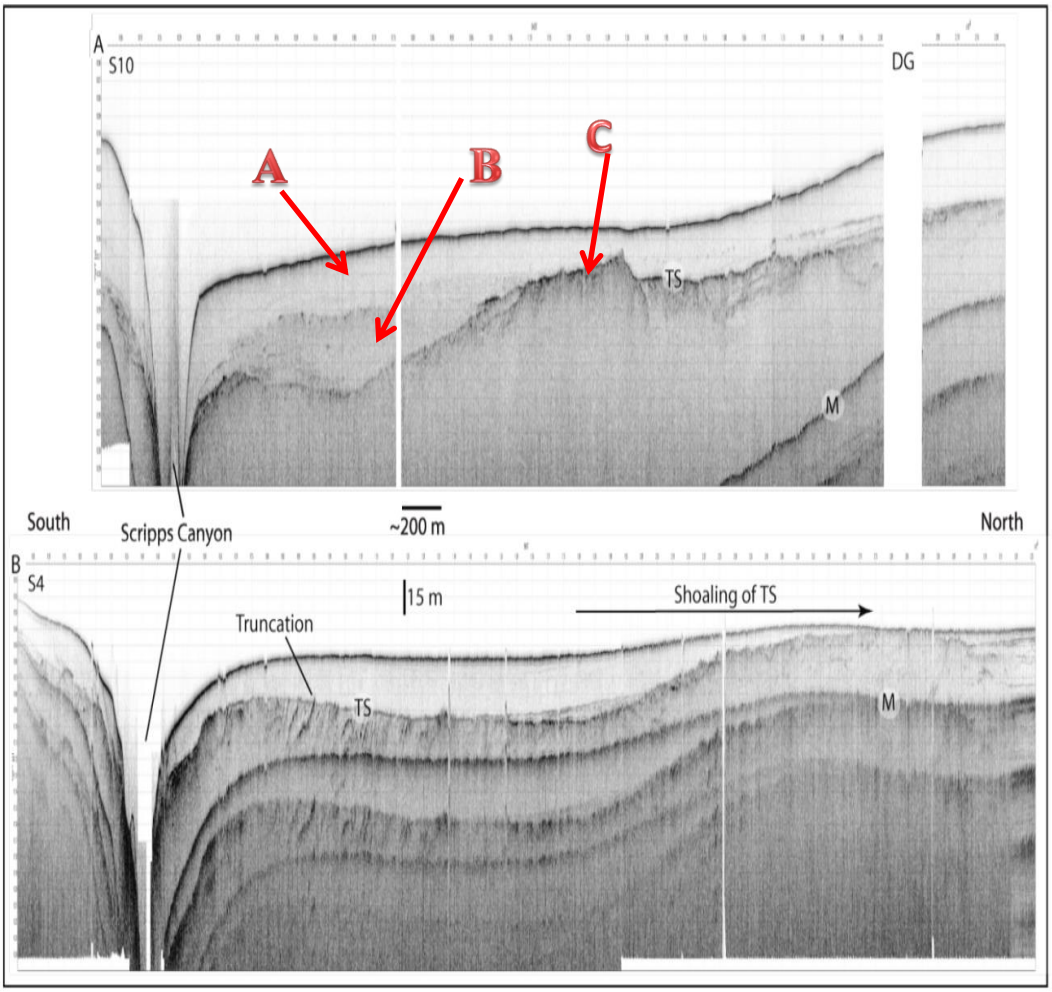


Figure 3. (Hogarth et al., 2007) Alongshore CHIRP seismic profile displaying three different stratigraphic facies. A) Modern Holocene sediments B). Basal lag deposit C). Truncated transgressive surface

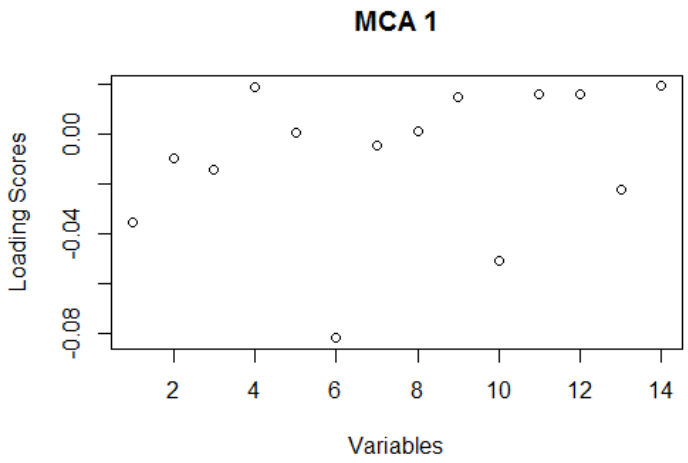


Figure 4. Component loading scores for first dimension of multiple correspondence analysis (MCA 1).

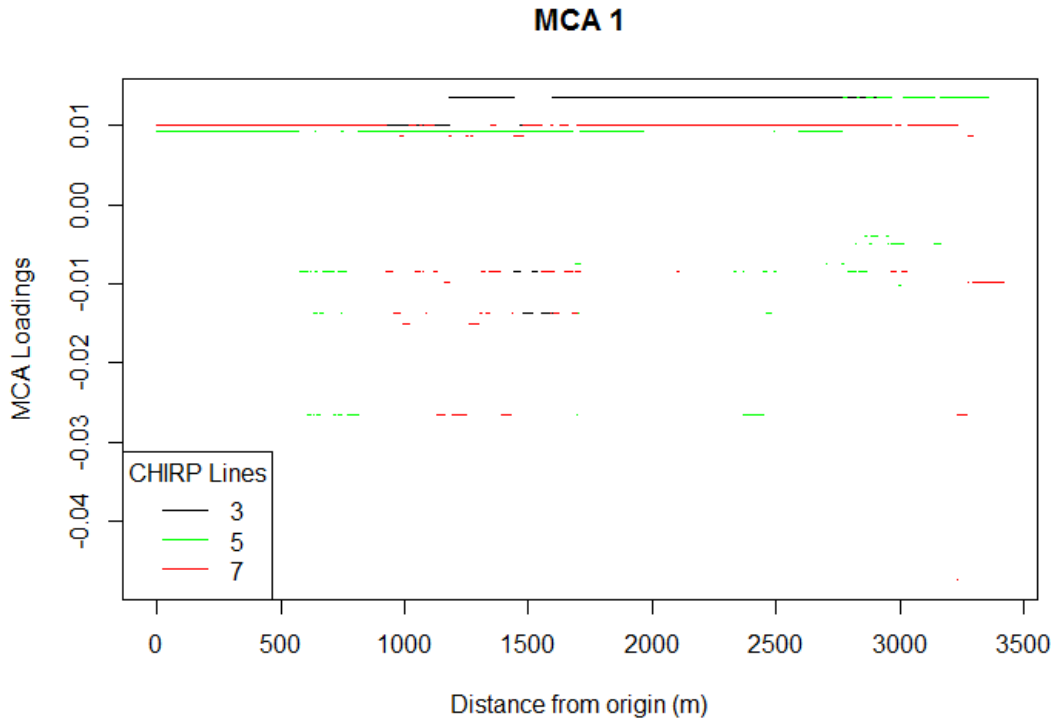


Figure 5. MCA 1 component loading scores for each individual CHIRP transect (3,5,7) as a function of distance from the origin.

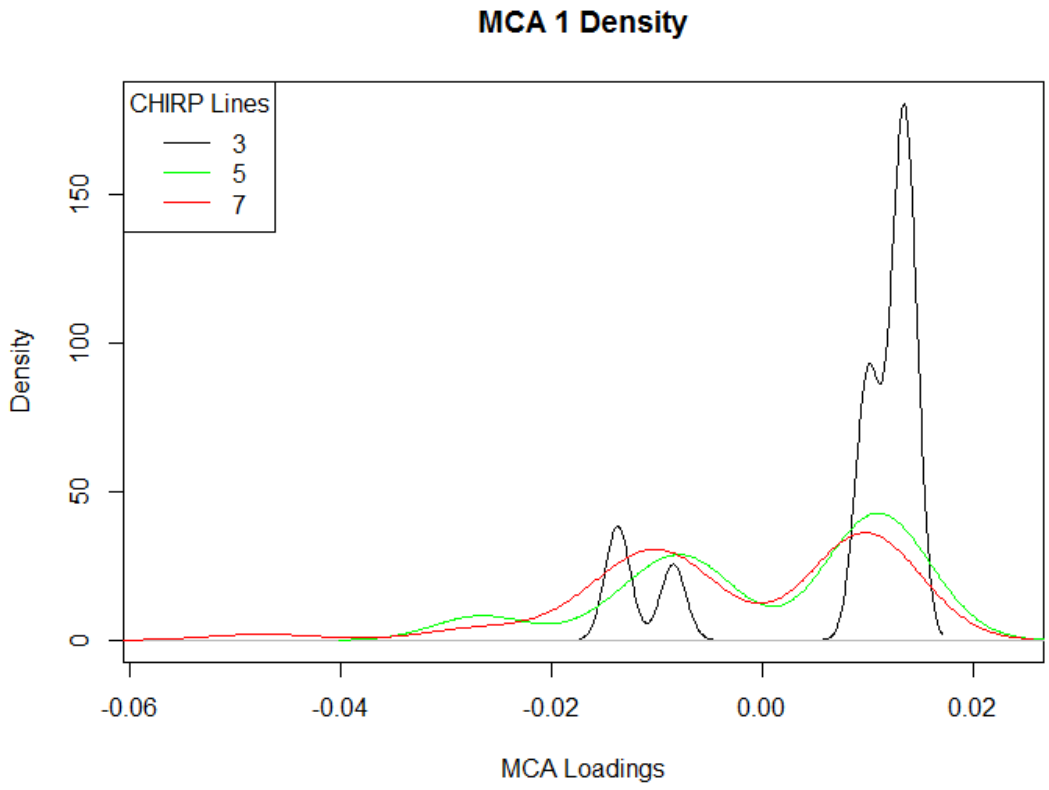


Figure 6. Density plot of component loading scores for the first dimension of multiple correspondence analysis (MCA1).

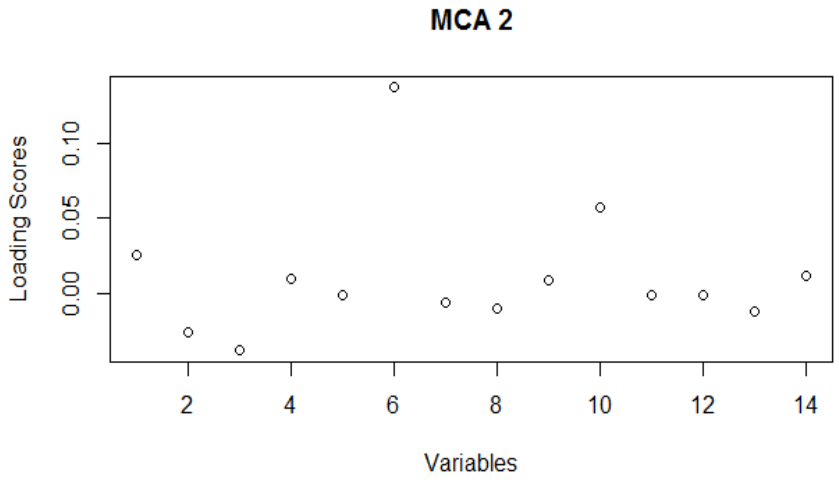


Figure 7. Component loading scores for second dimension of multiple correspondence analysis (MCA 2).

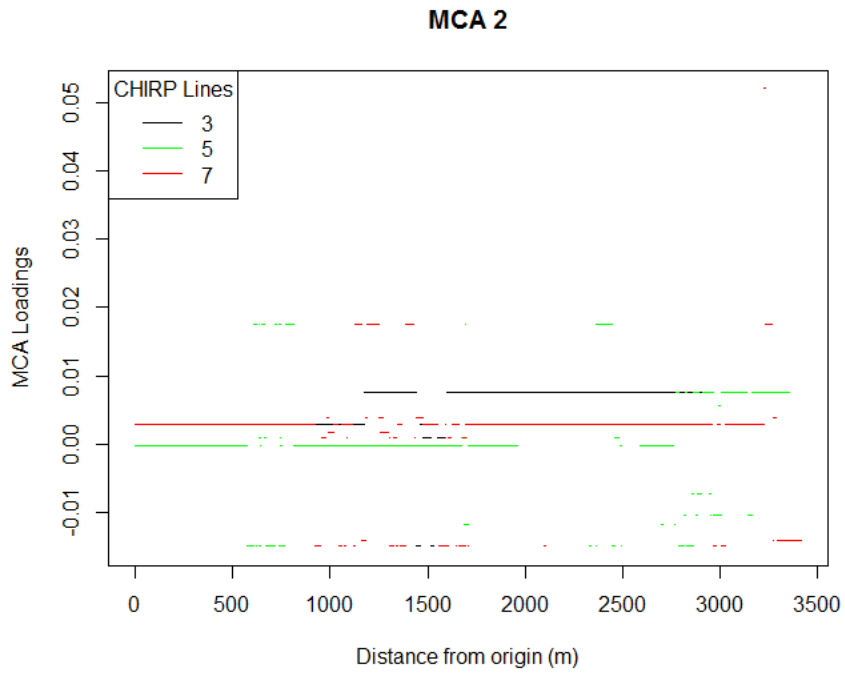


Figure 8. MCA 2 component loading scores for each individual CHIRP transect (3,5,7) as a function of distance from the origin.

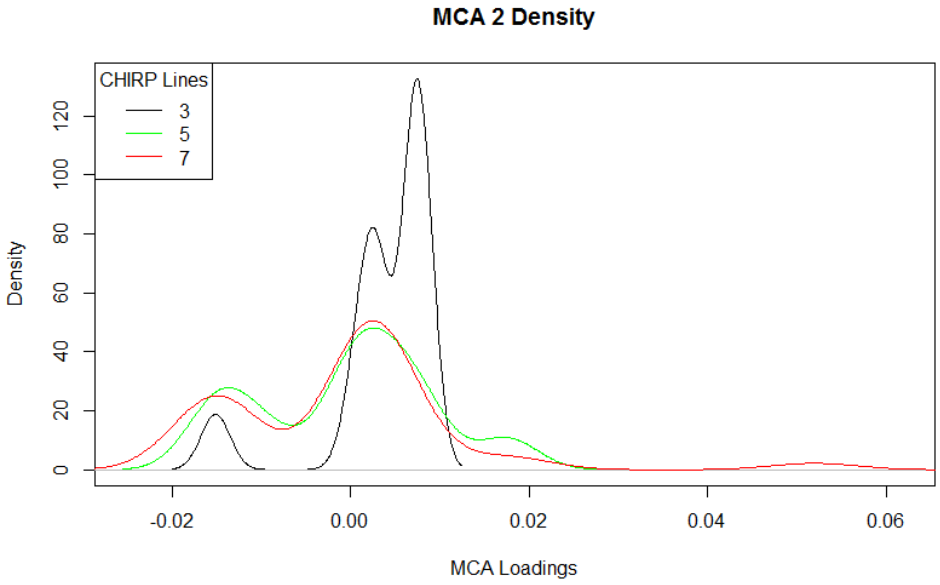


Figure 9. Density plot of component loading scores for the second dimension of multiple correspondence analysis (MCA 2).

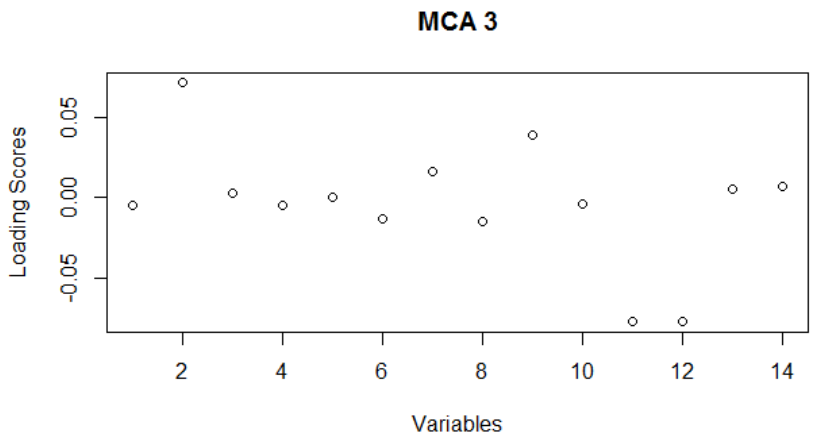


Figure 10. Component loading scores for the third dimension (MCA3) of multiple correspondence analysis.

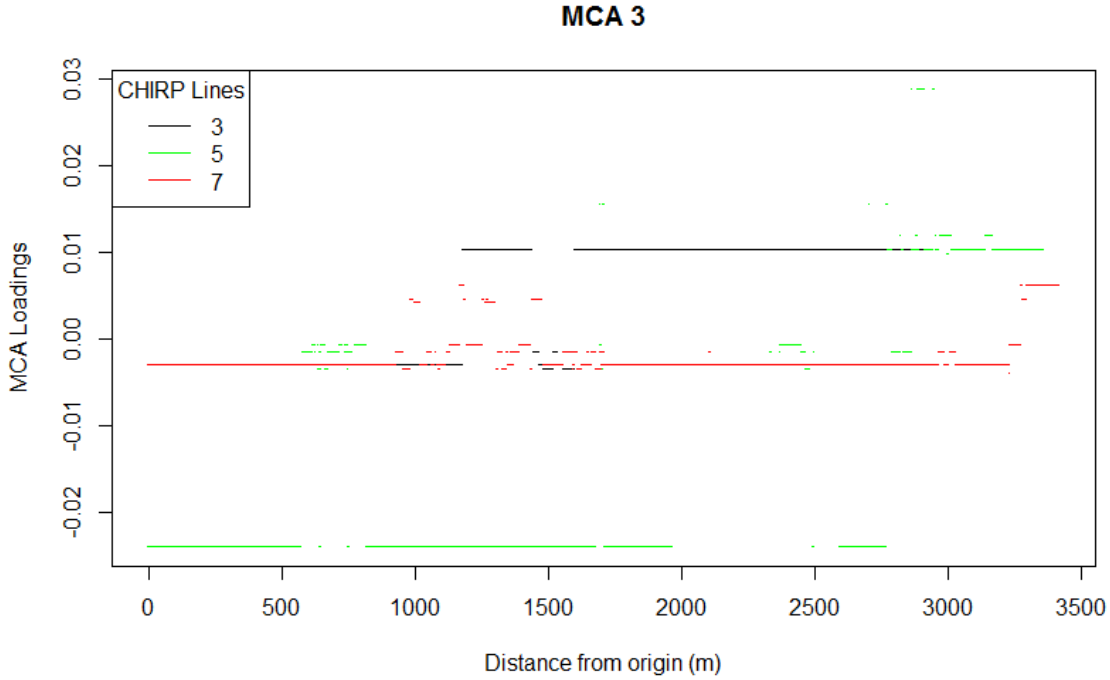


Figure 11. MCA3 component loading scores for each individual CHIRP transect as a function of distance from the origin.

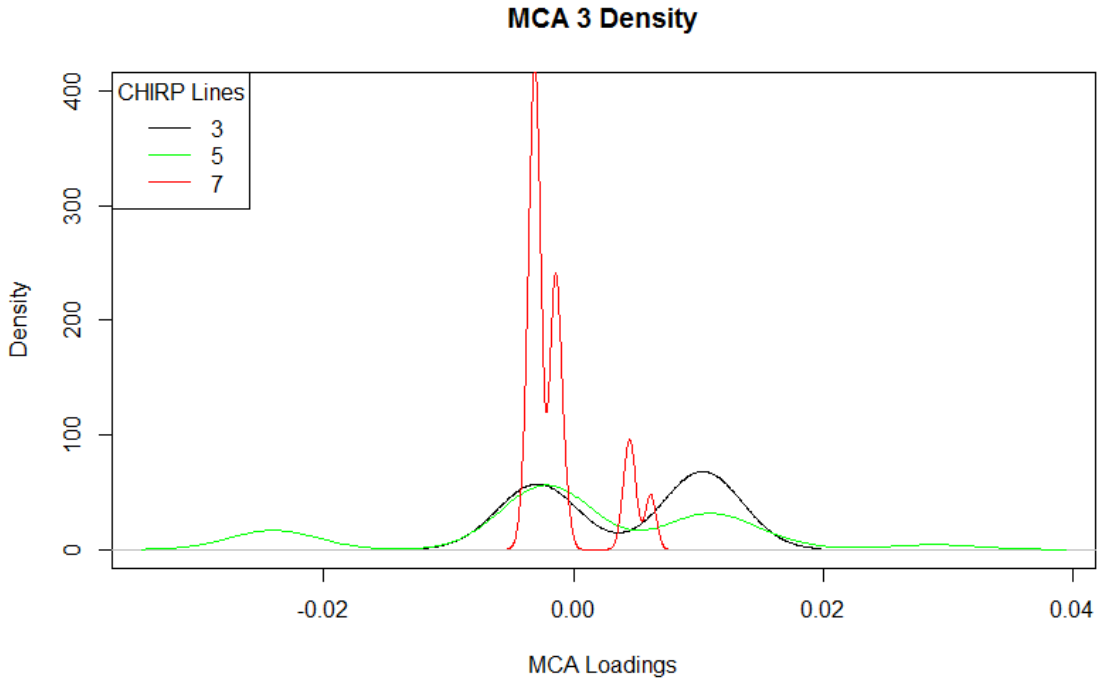


Figure 12. Density plot of component loading scores for the third dimension (MCA3) of multiple correspondence analysis.

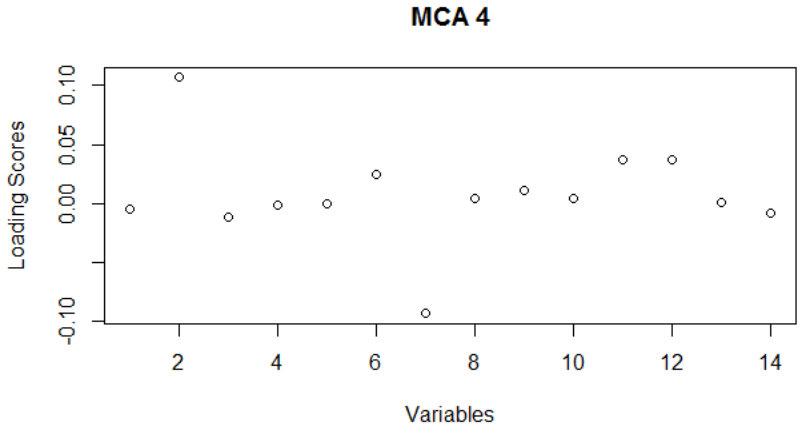


Figure 13. Component loading scores for the third dimension (MCA3) of multiple correspondence analysis.

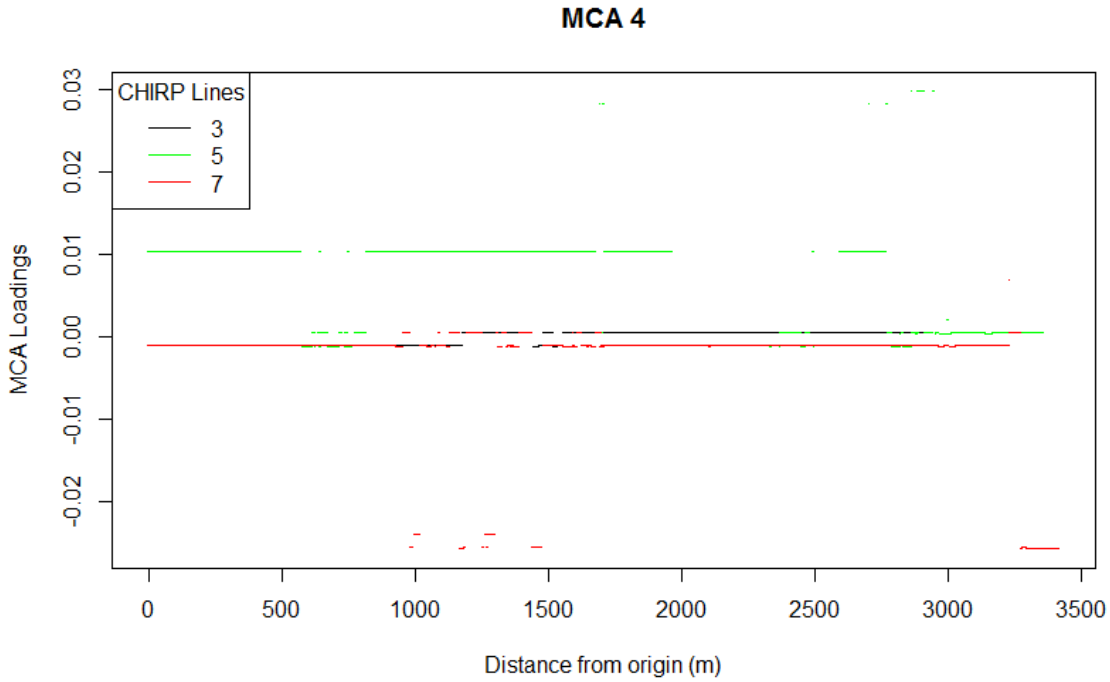


Figure 14. MCA 3 component loading scores for each individual CHIRP transect as a function of distance from the origin.

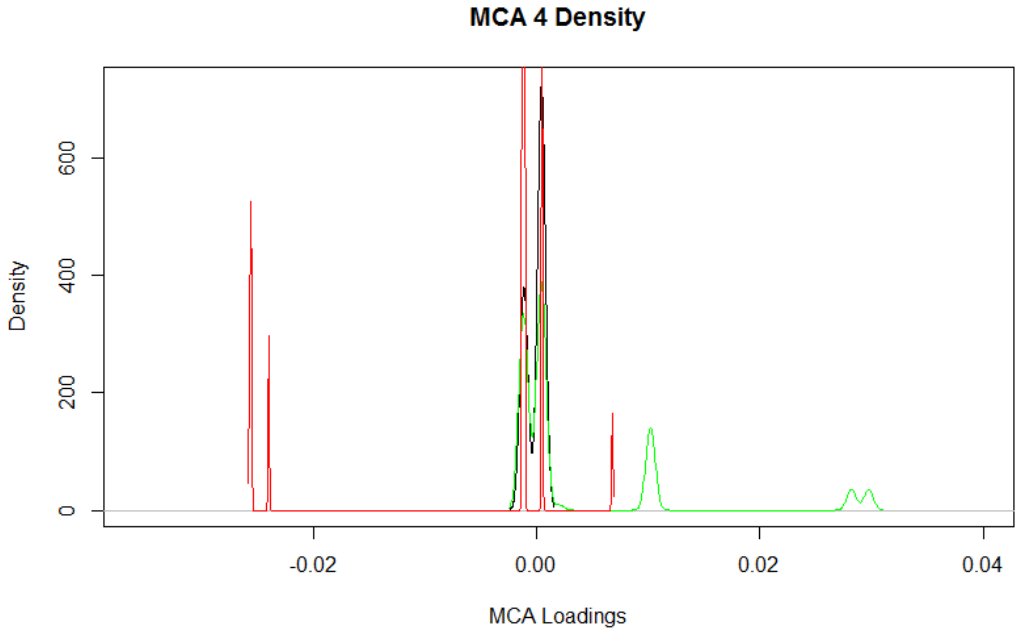


Figure 15. Density plot of component loading scores for the fourth dimension (MCA4) of multiple correspondence analysis.

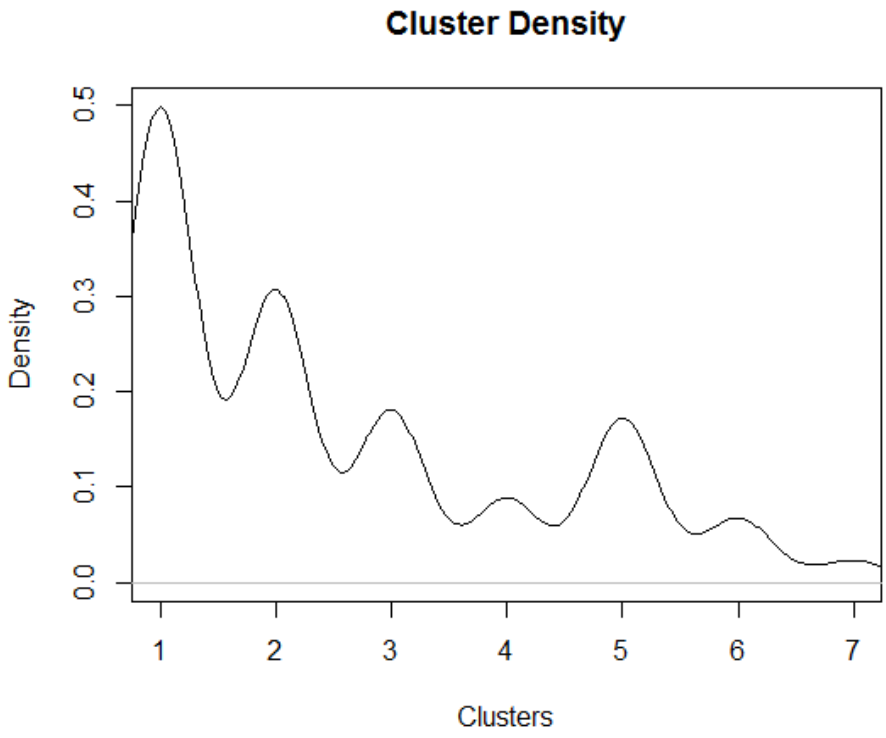


Figure 16: Density plot of cluster habitats on pooled CHIRP transect data.

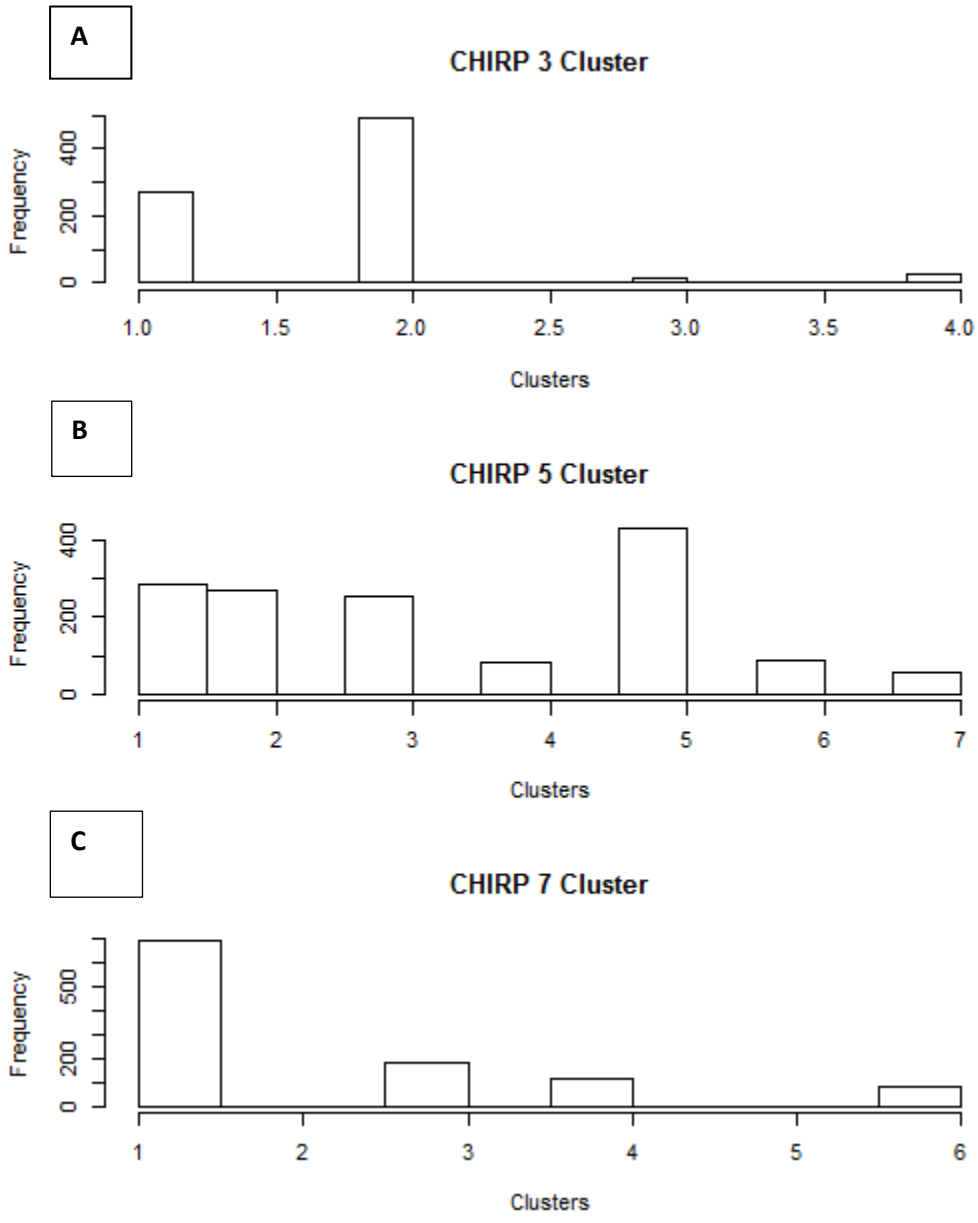


Figure 17. A). Cluster frequency along CHIRP 3. B). Cluster frequency along CHIRP 5. C). Cluster frequency along CHIRP 7.

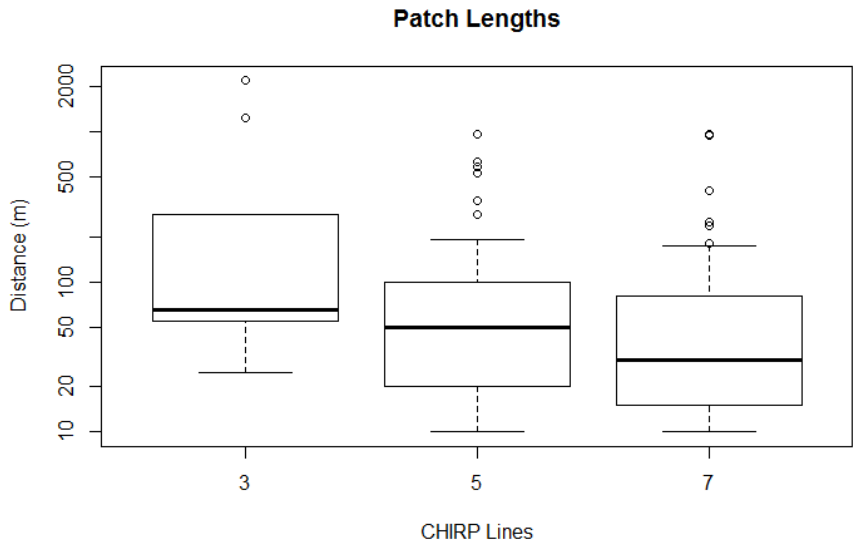


Figure 18. Average patch length box plot.

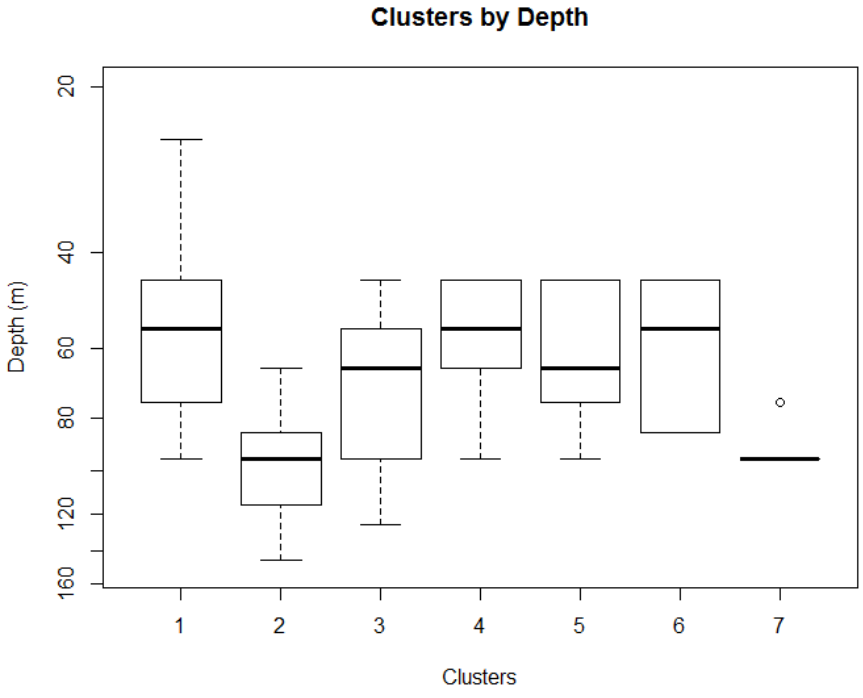


Figure 19. Individual clusters as a function of depth across all transects.

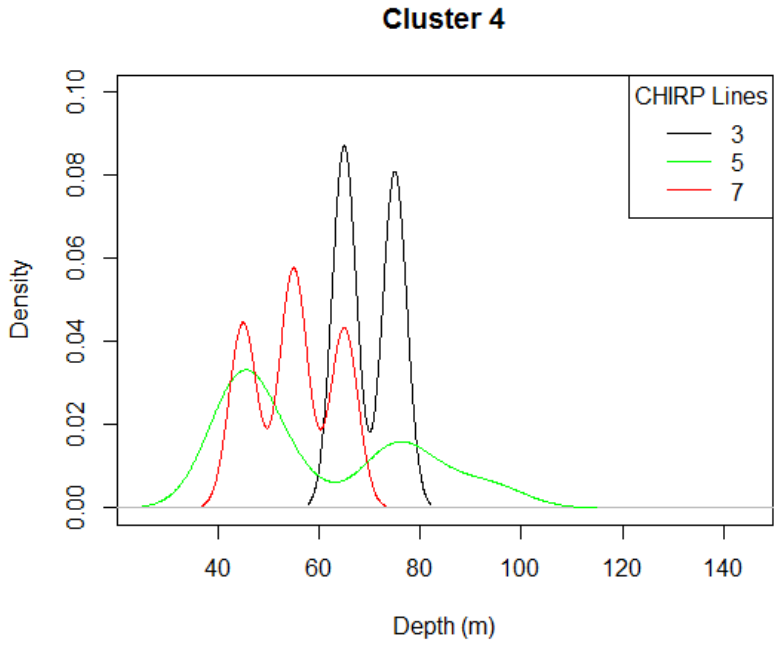


Figure 20. Cluster 4 density plot as a function of depth across all transects.

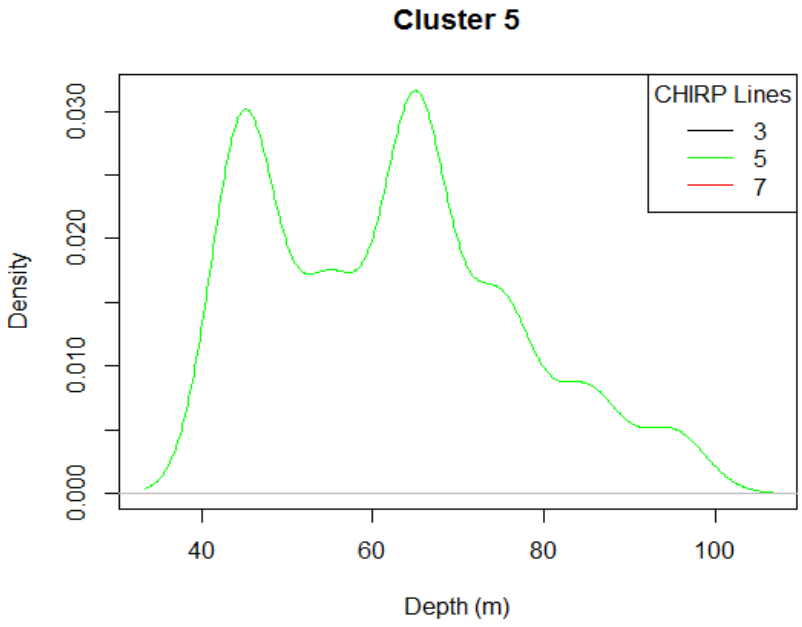


Figure 21. Cluster 5 density plot as a function of depth across all transects.

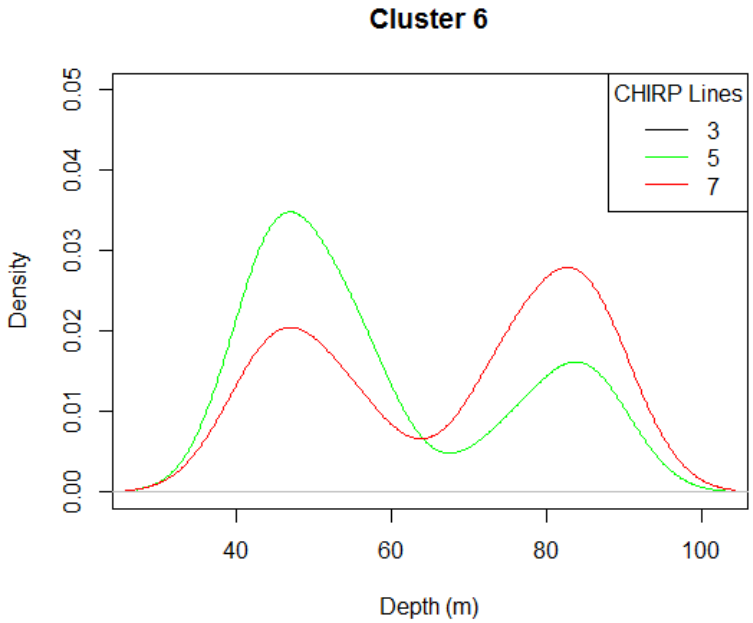


Figure 22. Cluster 6 density plot as a function of depth across all transects.

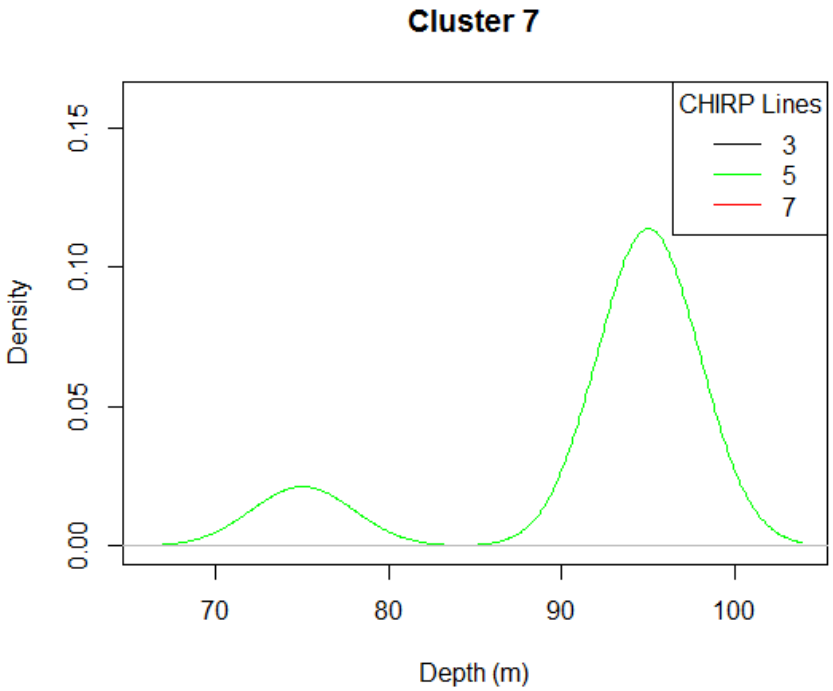


Figure 23. Cluster 7 density plot as a function of depth.

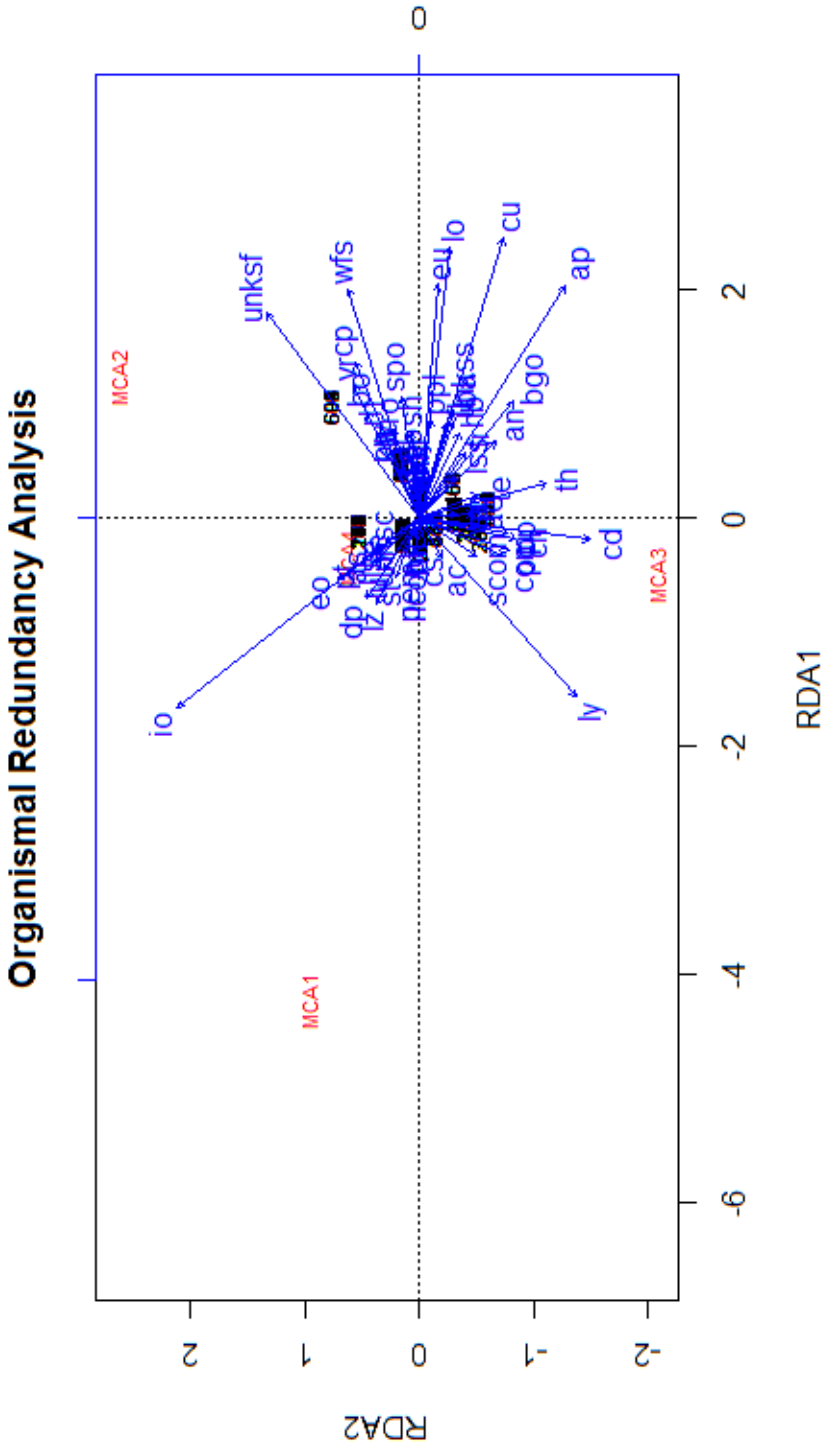


Figure 24. Biplot of organismal correlations with four MCA sites.

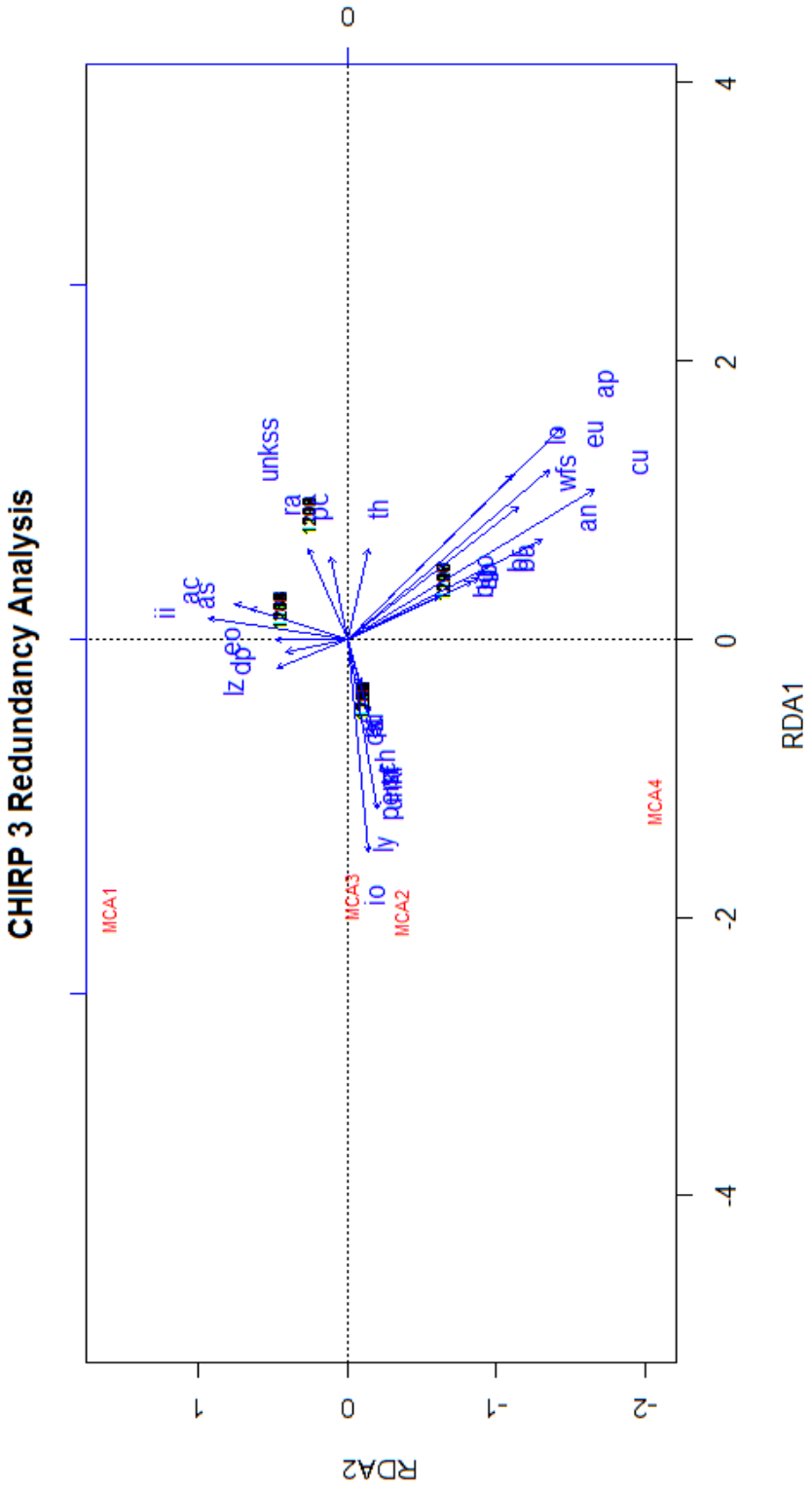


Figure 25. Biplot of organismal correlations with four MCA sites along CHIRP

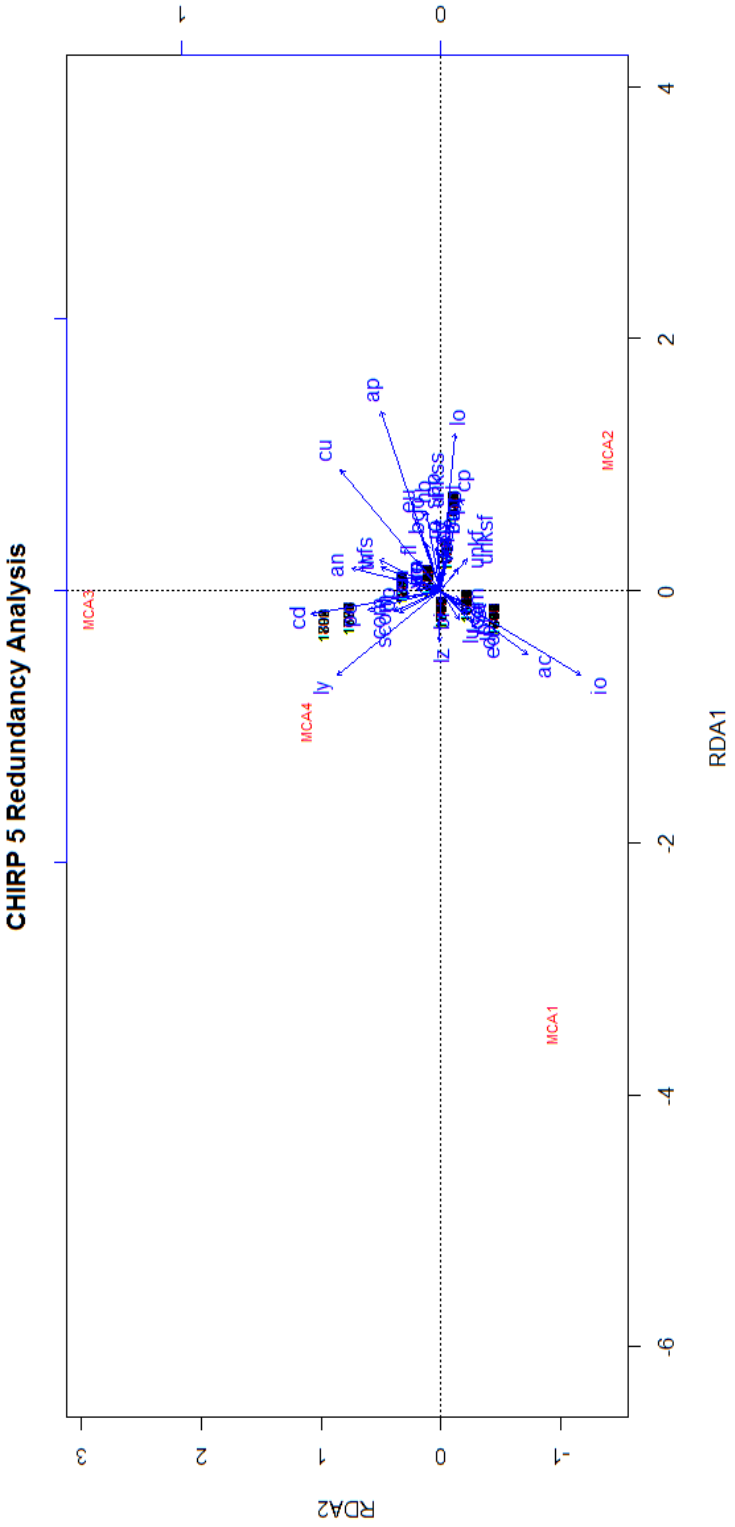


Figure 26. Biplot of organismal correlations with four MCA sites along CHIRP 5.

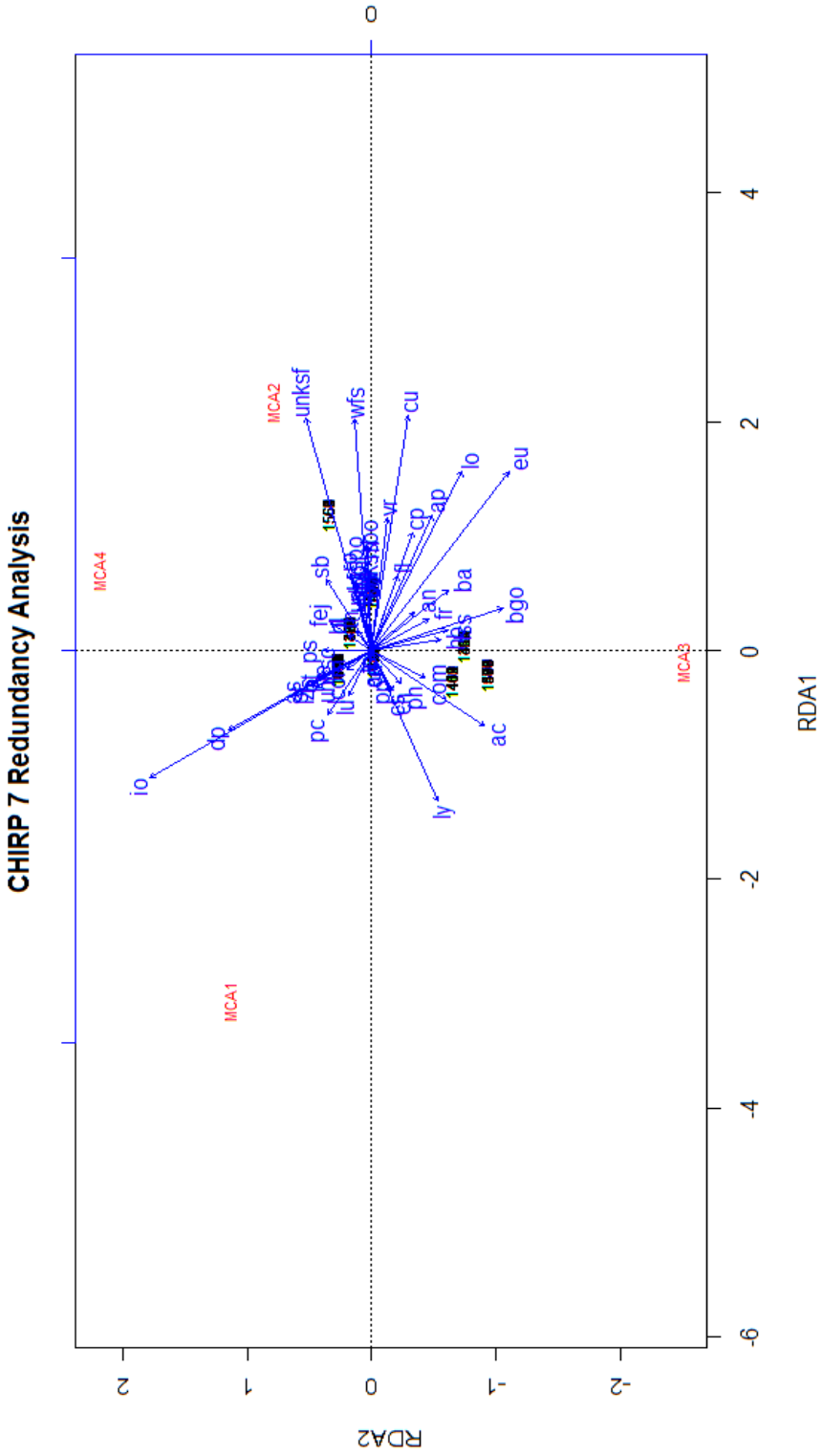


Figure 27. Biplot of organismal correlations with four MCA sites along CHIRP 7.

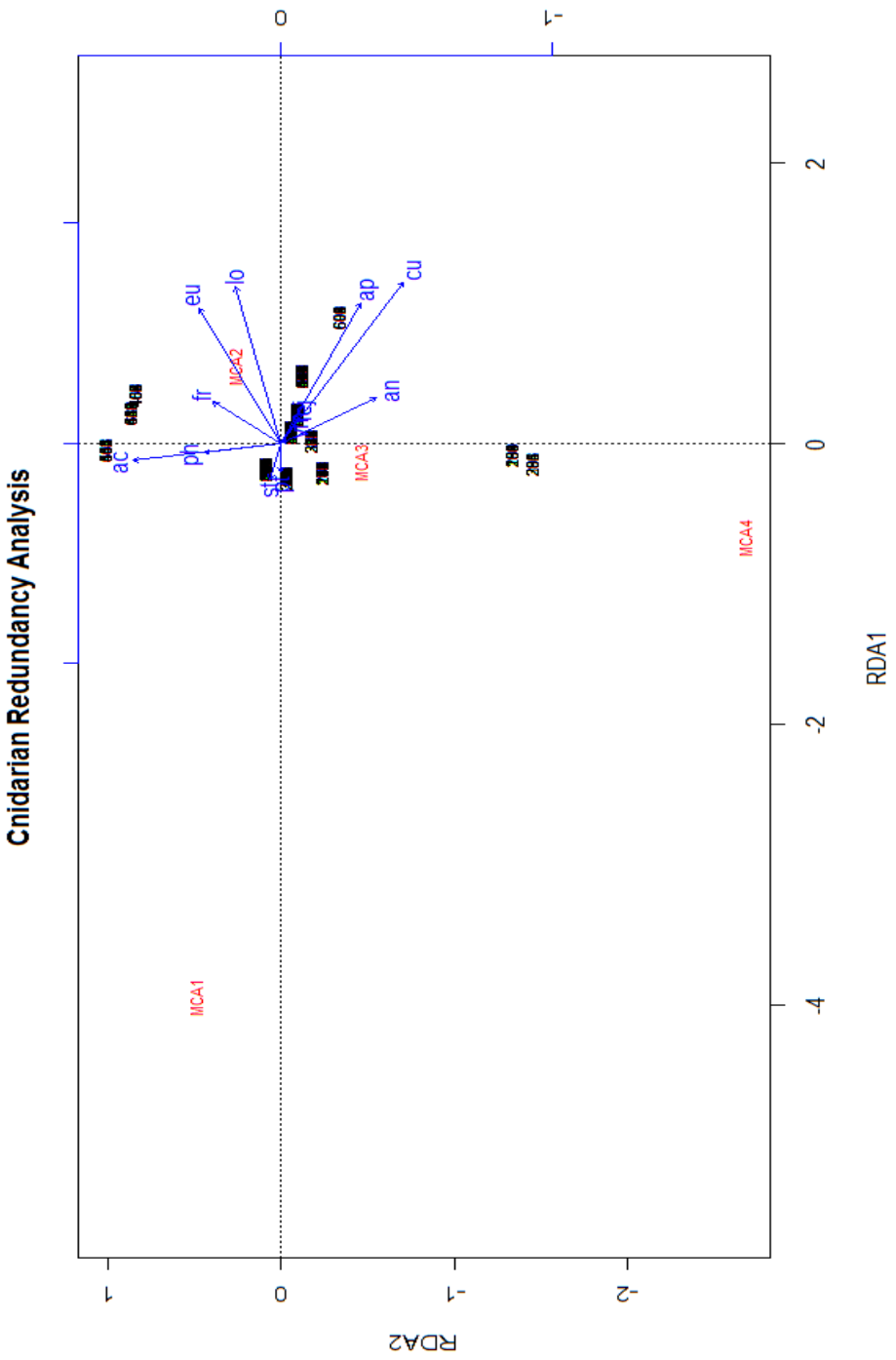


Figure 28. Biplot of Cnidarian correlations with four MCA sites along all transects.

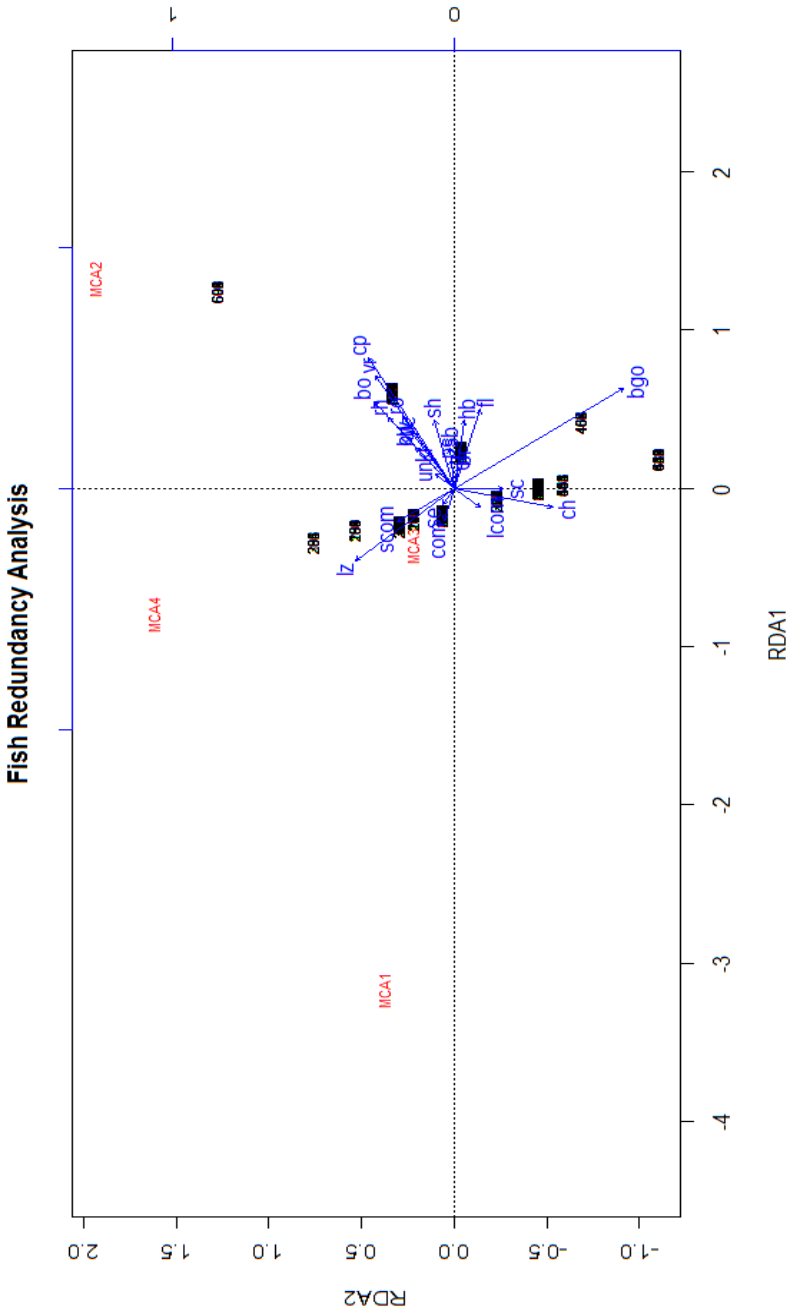


Figure 29. Biplot of fish correlations with four MCA sites along all transects

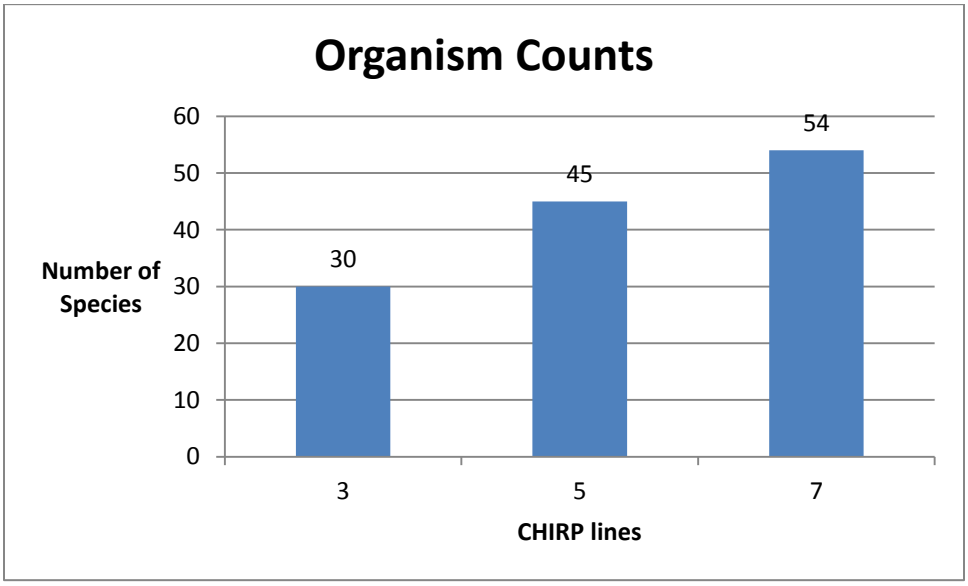


Figure 30. Histogram displaying increase in species richness as we move north along strike of the Rose Canyon Fault.

## Appendix

Table A-1. List of all organisms identified along pooled transect data.

| Organismal Code | Scientific Name | Common Name | Scale |
|---|---|---|---|
| cd | *Florometra serratissima* | Feather Star/Crinoid | Linear |
| io | | Infaunal ophiuroids | $Log_4$ |
| eo | *Amphioda luetkenii* | Epifaunal ophiuroids | $Log_4$ |
| ly | *Lytechinus anamesus* | White urchin | $Log_4$ |
| unku | | unknown urchin | Linear |
| pp | *Parastichopus parvimensis* | Warty sea cucumber | Linear |
| pc | *Parastichopus californicus* | California sea cucumber | Linear |
| unksc | | Unknown sea cucumber | Linear |
| lu | *Luidia foliolata* | Sand star | Linear |
| ls | *Luidia sarsi* | Sand star | Linear |
| as | *Astropecten armatus* | Spiny sand star | Linear |
| ba | *Asterina miniata* | Bat star | Linear |
| ra | *Orthasterias koehleri* | Rainbow star | Linear |
| pg | *Pisaster giganteus* | Giant sea star | Linear |
| ss | *Pisaster brevispinus* | Short-spined sea star | Linear |
| ae | *Mediaster aequalis* | Vermilion star | Linear |
| hl | *Henricia leviuscula* | Pacific blood star | Linear |
| unkss | | Unknown sea star | Linear |
| lss | *Dermasterias imbricate* | Leather star | Linear |
| bas | *Gorgonocephalus eucnemis* | Basket star | Linear |
| de | *Dendraster excentricus* | Sand dollar | $Log_4$ |
| ye | *Cancer anthonyi* | Yellow crab | Linear |
| shc | *Loxorhynchus gradis* | Sheep crab | Linear |
| pa | *Pagarus armatus* | Hermit crab | Linear |
| unkc | | unknown crab | Linear |

| | | | |
|---|---|---|---|
| pi | *Panulirus interruptus* | California spiny lobster | Linear |
| ms | *Hemisquilla ensigera californiensis* | Mantis shrimp | Linear |
| cg | *Muricea californica* | California golden gorgonian | Linear |
| eu | *Eugorgia rubens* | Purple gorgonian | Linear |
| lo | *Leptogorgia chilensis* | Red gorgonian | Linear |
| ap | *Adelogorgia phylloscera* | Orange gorgonian | Linear |
| fr | *Muricea fruticosa* | Brown gorgonian | Linear |
| an | *Parazoanthus lucificum* | Yellow zoanthid | Linear |
| ph | *Phyllactis sp.* | Sand Anemone | Linear |
| cu | *Balonophyllia elegans & Corynactis californica* | Cup Corals | $Log_4$ |
| fej | *Phacellophora camtschatica* | Fried egg jellyfish | Linear |
| pt | *Ptilosarcus gurneyi* | Orange sea pen | Linear |
| st | *Stylatula elongata* | White sea pen | Linear |
| vm | *Virgularia mirabilis* | Slender sea pen | Linear |
| ac | *Acanthoptilum gracile* | Graceful sea pen | Linear |
| pl | *Pleurobranchaea californica* | Sea slug | Linear |
| bi | *Octopus bimaculoides* | California two-spot octopus | Linear |
| ru | *Octopus rubescens* | East Pacific red octopus | Linear |
| sq | *Doryteuthis opalescens* | Market squid | Linear |
| li | *Lithopoma undosum* | Wavy turban snail | Linear |
| kw | *Kelletia kelletii* | Kellet's whelk | Linear |
| fo | *Fusitriton oregonensis* | Hairy triton snail | Linear |
| unksn | | Unknown snail | Linear |
| cs | *Conus californicus* | California cone | Linear |
| mr | *Mitra idae* | Episcopal miter | Linear |
| lc | *Ophiodon elongatus* | Lingcod | Linear |

| | | | |
|---|---|---|---|
| fl | *Sebastes rubrivinctus* | Flag rockfish | Linear |
| hc | *Sebastes umbrosus* | Honeycomb rockfish | Linear |
| vr | *Sebastes miniatus* | Vermilion rockfish | Linear |
| ro | *Sebastes rosaceus* | Rosy rockfish | Linear |
| sc | *Scorpaena guttata* | California scorpionfish | Linear |
| sh | *Semicossyphus pulcher* | Sheephead | Linear |
| ch | *Paralichthys californicus* | California halibut | Linear |
| ca | *Sebastes dallii* | Calico rockfish | Linear |
| ti | *Sebastes nigrocintus* | Tiger rockfish | Linear |
| cp | *Chromis punctipinnus* | Blacksmith fish | $Log_4$ |
| hb | *Sebastes semicinctus* | Halfbanded rockfish | $Log_4$ |
| unksf | | Unknown schooling fish | $Log_4$ |
| ep | *Family: Zoarcidae* | Eelpout | Linear |
| ow | *Caulolatilus princeps* | Ocean whitefish | Linear |
| ssd | *Citharichthys stigmaeus* | Speckled sand dab | Linear |
| tr | *Sebastes serriceps* | Tree rockfish | Linear |
| rw | *Halichoeres semicinctus* | Rock wrasse | Linear |
| bo | *Sebastes paucispinis* | Bocaccio | Linear |
| rh | *Rhacochilus toxotes* | Pile perch | Linear |
| se | *Oxyjulis californica* | Señorita fish | Linear |
| com | | Combfish | Linear |
| lcom | *Zaniolepis latipinnis* | Longspine combfish | Linear |
| scom | *Zaniolepis frenata* | Shortspine combfish | Linear |
| sb | *Sebastes spp.* | Rockfish | Linear |
| kb | *Paralabrax clathratus* | Kelp Bass | Linear |
| jm | *Trachurus symmetricus* | Pacific jack mackerel | $Log_4$ |
| ps | *Zalembius rosaceus* | Pink seaperch | Linear |
| spo | | Sponge | Linear |

| | | | |
|---|---|---|---|
| bs | *Cliona celata* | Boring sponge | Linear |
| wfs | *Toxadocia spp.* | White finger sponge | Linear |
| | | | |
| vs | Unknown species | Vase Sponge | Linear |
| te | *Tethya aurantium* | Orange puffball sponge | Linear |
| cr | *Craniella arb* | Gray puffball sponge | Linear |
| hal | *Haliclona spp.* | Demosponge | Linear |
| dp | *Diopatra spp.* | Polychaete worm | $Log_4$ |
| ppl | *Polyclinum planum* | Elephant ear tunicate | Linear |
| mse | *Naticidae spp.* | Moon snail egg casing | Linear |

## References


Buckingham, M.J. and Richardson, M.D., 2002. On tone-burst measurements of sound speed and attenuation in sandy marine sediments. IEEE *Journal of Oceanic Engineering*, 27 (3), 429-453.

Buhl-Mortensen, L., Vanreusel, A., Gooday, A.J., Levin, L.A. Priede, I.G., Buhl-Mortensen, P., Gheerardyn, H., King, N.J., & Raes, M., 2010. Biological strucutures as a source of habitat heterogeneity and biodiversity on the deep ocean margins. *Marine Ecology*, 31, 21-50.

Byrd, R.E., Berry, R.W., Fischer, P.J., 1975. Quaternary geology of the San Diego–La Jolla underwater park. Studies of the geology of Camp Pendelton and Western San Diego County, CA. San Diego Association of Geologists, 77–79.

Christie-Blick. and N., Driscoll, N.W., 1995, Sequence stratigraphy: *Annual Review of Earth and Planetary Sciences*, v. 23, p. 451-478.

Cimberg, R.L., Gerrodette T, & Muzik K., 1981. Habitat requirements and expected distribution of Alaska coral. Final Rep, VTN Oregon, Inc. Rep Office Marine Pollut Assess, Alaska Off, US Dept Commerce, NOAA, OCSEAP Final Rep 54: 207-308.

Darigo, N.J. and Osbourne, R.H., 1986. Quaternary stratigraphy and sedimentation of the inner continental shelf, San Diego County, California. Shelf sands and sandstones: In: Knight, R.J., McLean, J.R. (Eds.), Canadian Society of Petroleum Geologists Memoir II, 73–98.

Diaz, R. J., Solan, M., & Valente, R. M., 2004. A review of approaches for classifying benthic habitats and evaluating habitat quality. *Journal of environmental management*, *73*(3), 165–81. doi:10.1016/j.jenvman.2004.06.

Digby, P.G.N. and Kempton, R. A., 1987. Multivariate Analysis of Ecological Communities. Chapman and Hall, London - New York 1987, VIII, 206 S., £25 Biom. J., 32: 94. doi: 10.1002/bimj.4710320115.

Driscoll, N.W. and Hogg, J.R., 1995, Stratigraphic response to basin formation; Jeanne d'Arc Basin, offshore, Newfoundland, in Lambiase, J.J., ed., Hydrocarbon habitat in rift basins: Geological Society of London Special Publication 80, p. 145–163.

Emery, K.O., 1958. Shallow submerged marine terraces of Southern California. Geological Society of America Bulletin 69 (1), 39–60.

Engle, J.M., K.D., Lafferty, J.E., Dugan, D.L., Martin, N. Mode, R.F., Ambrose, & Raimondi, P.T., 1995. Second year study plan for inventory of coastal ecological resources of the northern Channel Islands and Ventura/Los Angeles Counties. California Coastal Commission Report. 46p.

Fairbanks, R.G., 1989. A 17,000-year glacio-eustatic sea-level record: influence of glacial melting rates on the Younger Dryas event and deep-ocean circulation. *Nature* 342, 637–642.

Fischer, P. J. and Mills, G.I., 1991. The offshore Newport–Inglewood–Rose Canyon fault zone, California: structure, segmentation and tectonics, in Environmental Perils San Diego Region, P. L. Abbott and W. J. Elliot (Editors), San Diego Association of Geologists, San Diego, Geological Society of America Annual Meeting, 17–36.

Flick, R.E., 1993. The myth and reality of Southern California beaches. Shore & Beach, July 1993, 3–13.

Flick, R.E., 1994. Shoreline Erosion Assessment and Atlas of the San Diego Region. Sacramento, California: California Department of Boating and Waterways, 2 volumes.

Grant, L.B. and Shearer, P., 2004. Activity of the Offshore Newport–Inglewood Rose Canyon Fault Zone, Coastal Southern California, from Relocated Microseismicity Bulletin of the Seismological Society of America, Vol. 94, 747–752.

Hass, J.K., 2005. Grain size and mineralogical characteristics of beach sand in the Oceanside Littoral Cell, Southern California: implications for sediment provenance.Thesis (M. S.)–University of California, San Diego.

Henry, M.J., 1976. The unconsolidated sediment distribution on the San Diego County mainland shelf, California. Masters thesis, San Diego State University.

Hogarth, L. J., Babcock, J., Driscoll, N. W., Le Dantec, N., Haas, J. K., Inman, D. L. & Masters, P. M., 2007. Long-term tectonic control on Holocene shelf sedimentation offshore La Jolla, California. *Geology*, *35*(3), 275. doi:10.1130/G23234A.1

Hutchinson, G.E., 1957. "Concluding remarks" (PDF). *Cold Spring Harbor Symposia on Quantitative Biology* **22** (2): 415–427. doi:10.1101/sqb.1957.022.01.039.

Ierodiaconou, D., Monk, J., Rattray, A., Laurenson, L., & Versace, V.L., 2011. Comparison of automated classification techniques for predicting benthic biological communities using hydroacoustics and video observations. *Continental Shelf Research*, *31*(2), S28–S38. doi:10.1016/j.csr.2010.01.012

Inman, D.L. and Chamberlain, T.K., 1960. Littoral sand budget along the southern California coast. Volume of Abstracts, Report of the 21st International Geological Congress, Copenhagen, Denmark, 245–246.

Jackson, J.B.C., Budd, A.F., & Pandolfi, J.M., 1996. The shifting balance of natural communities. In: Jablouski D, Erwin DH, Lipps, JH (eds) Evolutionary paleobiology, University of Chicago Press, Chicago, 89-122.

Johannes, R., 1974. Sources of nutritional energy for reef corals. Proc. Int. Coral Reef Symp. (2nd) v. 1, 133-137. Great Barrier Reef Committee, Brisbane.

Kennedy, M.P., 1975. Western San Diego metropolitan area: Del Mar, La Jolla, and Point Loma, 7 1/2 minute quadrangles. Bulletin, California, Division of Mines and Geology, vol. 200, 9–39.

Kennedy, M.P. and Moore, G.W., 1971. Stratigraphic relations of Upper Cretaceous and Eocene formations, San Diego coastal area, California: Am. Assoc. Petroleum Geologists Bull., v. 55, p. 709-722.

Kostylev, V.E., Todd, B.J., Fader, G.B.J., Courtney, R.C., Cameron, G.D.M., & Pickrill, R.A., 2001. Benthic habitat mapping on the Scotian Shelf based on multibeam bathymetry, surficial geology and sea floor photographs. *Marine Ecology Progress Series* 219, 121-137.

Le Dantec, N., Hogarth, L. J., Driscoll, N.W., Babcock, J. M., Barnhardt, W. A. & Schwab, W. C., 2010. Tectonic controls on nearshore sediment accumulation and submarine canyon morphology offshore La Jolla, Southern California. *Marine Geology*, *268*(1-4), 115–128. doi:10.1016/j.margeo.2009.10.026

Legendre, P. and Legendre, L., 2012. Numerical ecology, 3rd English edition. Developments in Environmental Modelling, Vol. 24. Elsevier Science BV, Amsterdam. xiv + 990 pp. ISBN-13: 978-0444538680. http://www.elsevierdirect.com/ISBN/9780444538680/Numerical-Ecology

Legendre, P. and Anderson M.J., 1999. Distance-based redundancy analysis: testing multispecies responses in multifactorial ecological experiments. Ecological Monographs 69:1–24.

Levin, L.A., Etter, R. J., Rex, M. A., Gooday, A. J., Smith, C. R., Pineda, J., Stuart, C.T., Hessler, R.R., & Pawson, D., 2001. Environmental influences on regional deep-sea species diversity. Annual Review of Ecology and Systematics. 32:51-93.

Lewis, J. B. and Price, W.S., 1975. Feeding mechanisms and feeding strategies of Atlantic reef corals. *Journal of Zoology*, 176: 527–544. doi: 10.1111/j.1469-7998.1975.tb03219.x

Lewis, J. B. and Price, W. S. 1976. Patterns of ciliary currents in Atlantic reef corals and their functional significance. Journal of Zoology, 178: 77–89. doi: 10.1111/j.1469-7998.1976.tb02264.x

Lindvall, S. C. and Rockwell, T.K., 1995, Holocene activity of the Rose Canyon fault zone in San Diego, California, *J. Geophys. Res*., 100(B12), 24121–24132, doi:10.1029/95JB02627.

MacArthur, R. H. and Wilson, E.O., 1963 An Equilibrium Theory of Insular Zoogeography Evolution Vol. 17, No. 4. 373-387 http://www.jstor.org/stable/2407089

MacArthur, R. H. and Wilson, E.O., 1967. The Theory of Island Biogeography. Princeton, N.J.: Princeton University Press.

Mortensen, P.B., 2001. Aquarium observations on the deep-water coral *Lophelia pertusa* (L., 1758) (Scleractinia) and selected associated invertebrates. Ophelia 54(2): 83- 104.Thesis (M. S.)–University of California, San Diego.

Muscatine, L., 1973. Nutrition of corals. pp. 77–115. in: Jones, O. A., and R. Endean (eds.), The Biology and Geology of Coral Reefs. Vol. 2, Biology I. Academic Press, New York. 77-115.

Nummedal, D. and Swift, D.J.P., 1987. Transgressive stratigraphy at sequence-bounding unconformities: Some principles derived from Holocene and Cretaceous examples, in Nummedal, D., Pilkey, O.H., and Howard, J.D., eds., Sea-level fluctuation and coastal evolution: Society of Economic Paleontologists and Mineralogists Special Publication 41. P. 241-260.

Orange, D.L., 1999, Tectonics, sedimentation, and erosion in northern California; submarine geomorphology and sediment preservation potential as a result of three competing processes; The formation of continental-margin strata: *Marine Geology*, v. 154, p. 369–382, doi:10.1016/S0025–3227(98)00124–8.

Pirtle, J.L., 2005. Habitat-based assessment of structure-forming megafaunal invertebrates and fishes on Cordell Bank, California. M.Sc. Thesis, Washington State Univ., Vancouver, Washington, USA, 64pp.

Posamentier, H.W., and Allen, G.P., 1999. Siliciclastic sequence stratigraphy: concepts and applications. SEPM, Concepts in Sedimentology and Paleontology, vol. 7. 210 pp.

Quinn, G.P. and Keough, M.J., 2002. Experimental Design and Data Analysis for Biologists Cambridge University Press , 537 pp.

R Core Team., 2012. R: A language and environment for statistical computing. R Foundation for Statistical Computing, Vienna, Austria. ISBN 3-900051-07-0, URL http://www.R-project.org/

Rentz, P.T., 2010. The influence of tectonics, sea level, and sediment supply on coastal morphology in the Oceanside littoral cell, CA. UC San Diego: b6940598. Retrieved from: http://escholarship.org/uc/item/3rc16754

Shepard, F.P. and Inman, D.L., 1950. Nearshore water circulation related to bottom topography and wave refraction. Transactions of the American Geophysical Union 31 (2), 196–212.

Silvertown J., 2004. The ghost of competition past in the phylogeny of island endemic plants. *Journal of Ecology* 92: 168–173.

Sommerfield, C.K. and Lee, H.J., 2003. Magnitude and variability of Holocene sediment accumulation in Santa Monica Bay, California. Marine Environmental Research 56, 151–176.

Sommerfield, C.K. and Lee, H.J., 2004. Across-shelf sediment transport since the Last Glacial Maximum, southern California margin. *Geology* 32 (4), 345–348.

Sponaugle, S. and LaBarbera, M., 1991. Drag-induced deformation: a functional feeding strategy in two species of gorgonians. *J Exp Mar Biol Ecol* 148:121-134.

Sponaugle, S., 1991. Flow patterns and velocities around a suspension-feeding gorgonian polyp: evidence from physical models. *J Exp Mar Biol Ecol* 148:135-145.

Stow, D.A. and Chang, H.H., 1987. Coarse sediment delivery by coastal streams to the Oceanside Littoral Cell, California. Shore and Beach 55 (1), 30–40.

Thomson, J., Elgar, S. & Herbers, T.H.C., 2005. Reflection and tunneling of ocean waves observed at a submarine canyon. Geophysical Research Letters 32 (10), L10602.

Valladares, G., Salvo, A. & Cagnolo, L. (2006) Habitat fragmentation effects on trophic processes of insect–plant food webs.*Conservation Biology*, 20, 212–217.

Van Den Wollenberg, A., 1977. Redundancy analysis: An alternative for canonical correlation analysis Psychometrika, 42, 207–219.

Waggoner, J.A., 1979. Unconsolidated shelf sediments in the area of Scripps and La Jolla submarine canyons. Masters of Science in Geology, San Diego State University.

Walls, C., T. Rockwell, K. Mueller, Y. Bock, S. Williams, J. Pfanner, J. Dolan, & Feng, P., 1998. Escape tectonics in the Los Angeles metropolitan region and implications for seismic risk, *Nature* 394, 356– 360.

Whittaker, R.H., S.A. Levin, & Root, R.B., 1973. Niche, Habitat, and Ecotope. *The American Naturalist* 107(955):321–338.

Williams, K.L., Jackson, D.R., Thorsos, E.I., Tang, D. & Schock, S.G., 2002. Comparison ofsound speed and attenuation measured in a sandy sediment to predictions based on the Biot theory of porous media. IEEE *Journal of Oceanic Engineering* 27 (3), 413.

Willis, C.M. and Griggs, G.B., 2003. Reductions in fluvial sediment discharge by coastal dams in California and implications for beach sustainability. *Journal of Geology*, 111, 167–182.

Wright, T. L., 1991. Structural geology and tectonic evolution of the Los Angeles basin, In *Active Margin Basins*, K. T. Biddle (Editor), American Association of Petroleum Geologists Memoir 52, 35–134.

Young, A.P. and Ashford, S.A., 2006. Application of airborne LIDAR for seacliff volumetric change and beach-sediment budget contributions. *Journal of Coastal Research* 22 (2), 307–318.

Young, A., Olsen, M., Driscoll, N., Flick, R., Gutierrez, R., Guza, R. & Johnstone, E., 2010. Comparison of Airborne and Terrestrial Lidar Estimates of Seacliff Erosion in Southern California. Photogrammetric Engineering and Remote Sensing vol. 76, p. 421-427.

Young, A.P., Raymond, J.H., Sorenson, J., Johnstone, E.A., Driscoll, N.W., Flick, R.E. & Guza, R.T., 2010. Coarse Sediment Yields from Seacliff Erosion in the Oceanside Littoral Cell. Journal of Coastal Research. 26:580-585.